molecules

MDPI

Review

Liquid–Liquid and Liquid–Solid Interfacial Nanoarchitectonics

Katsuhiko Ariga [1,2]

[1] Research Center for Materials Nanoarchitectonics (MANA), National Institute for Materials Science (NIMS), Ibaraki 305-0044, Japan; ariga.katsuhiko@nims.go.jp
[2] Graduate School of Frontier Sciences, The University of Tokyo, Chiba 277-8561, Japan

Abstract: Nanoscale science is becoming increasingly important and prominent, and further development will necessitate integration with other material chemistries. In other words, it involves the construction of a methodology to build up materials based on nanoscale knowledge. This is also the beginning of the concept of post-nanotechnology. This role belongs to nanoarchitectonics, which has been rapidly developing in recent years. However, the scope of application of nanoarchitectonics is wide, and it is somewhat difficult to compile everything. Therefore, this review article will introduce the concepts of liquid and interface, which are the keywords for the organization of functional material systems in biological systems. The target interfaces are liquid–liquid interface, liquid–solid interface, and so on. Recent examples are summarized under the categories of molecular assembly, metal-organic framework and covalent organic framework, and living cell. In addition, the latest research on the liquid interfacial nanoarchitectonics of organic semiconductor film is also discussed. The final conclusive section summarizes these features and discusses the necessary components for the development of liquid interfacial nanoarchitectonics.

Keywords: covalent organic framework; liquid–liquid interface; liquid–solid interface; living cell; metal-organic framework; molecular assembly; nanoarchitectonics; organic semiconductor

Citation: Ariga, K. Liquid–Liquid and Liquid–Solid Interfacial Nanoarchitectonics. *Molecules* **2024**, *29*, 3168. https://doi.org/10.3390/molecules29133168

Academic Editor: Guanying Li

Received: 14 June 2024
Revised: 1 July 2024
Accepted: 2 July 2024
Published: 3 July 2024

1. Introduction

The world moves quickly, and various problems appear successively. Science and technology must keep up in finding solutions to these problems. Research on energy [1–10], environmental [11–20], and biomedical problems [21–30] is being conducted, spanning basic and applied perspectives. In addition, basic research and the development of devices that contribute to information technology are being conducted to build a new society [31–40]. To address these issues, it is essential to develop precisely organized functional materials. Mankind is tackling this problem tirelessly. Yet, the mechanisms to deal with these problems already exist in biological systems. Biological systems are very efficient and highly selective. Moreover, they operate under mild conditions and normal temperature and pressure. The secret is that in a biofunctional system, functional components are very intricately organized [41–44]. They work in tandem to achieve high functionality. A pre-existing methodology is there for reference. Living systems have developed such excellent systems over billions of years of evolution, and even though their organizational structures are highly diverse, there are a few common features. One is that they are constructed in liquid systems (aqueous solution systems). In living organisms, all functions occur in aqueous environments. Another feature is the use of interfaces. Biological mechanisms rarely take place in free solution. They always work at interfaces, such as cell membrane surfaces, the internal surfaces of protein pockets, and surfaces of biopolymers such as DNA. In other words, the key to the organization and expression of high functions in biological systems is twofold: the fact that they take place in liquid and in interfacial environments. The need for materials design to take advantage of these characteristics in artificial systems will be reiterated later in this introductory section. Liquid–liquid interfaces and liquid–solid interfaces are the key.

In comparison to the development of functional structures in living systems, which has developed over billions of years, humans have developed methodologies for creating functional materials in a much shorter time. Let us take a brief look at the development of materials by mankind. The development of human society depends on the materials that become available and the tools made from them. It was not until the 20th century that the methods of material creation were systematized as a discipline. The 20th century saw the systematization of the methods of substance creation as a discipline, the inception and development of various types of chemistry. In particular, the development of material chemistry owes much to the development of chemistry, which involves making various things from molecules. In addition, the development of physics to evaluate the fabricated materials was also essential. Furthermore, the development of biology, which deepens our relationship with nature, is also important to utilize science and technology for our daily life and health. Among these, chemistry, which makes materials, continues to develop new functional materials even today. Organic chemistry [45–54], inorganic chemistry [55–64], polymer chemistry [65–74], supramolecular chemistry [75–84], co-ordination chemistry [85–94], biochemistry [95–104], and other material chemistry [105–114] are still creating various new substances, systems, and principles. At the same time, physical chemistry [115–118], analytical chemistry [119–123], and interfacial chemistry [124–128] also continue to develop, in addition to physical methods for material properties [129–132]. Throughout this historical development, there is one fact that physics and chemistry have elucidated. It is the principle that properties and functions depend not only on the nature of the substance itself, but also on its external and internal structures [133–135]. In other words, control of structure and organization is essential for better functionality. In particular, control of the structure at the nanoscale level is crucial.

The founding of nanotechnology was pivotal in this research trend. Nanotechnology plays a central role in modern chemistry and is involved in various sciences and technologies. The observation of structure and motion at the atomic, molecular, and nanolevel [136–139], as well as the elucidation of specific physical properties in such small areas [140–143], are being studied. As these studies progress, the importance of nanoscale science is becoming increasingly prominent. Once the importance of nanoscale phenomena is well understood, it must be integrated with other material chemistries. This is the integration of understanding at the nanoscale with the technology of materials science. In other words, it is the construction of a methodology to build up materials based on nanoscale knowledge. This is also the beginning of the concept of post-nanotechnology [144]. This role is played by the concept of nanoarchitectonics, which has been rapidly developing in recent years. Just as Richard Feynman founded nanotechnology in the middle of the 20th century [145,146], nanoarchitectonics was proposed by Masakazu Aono at the beginning of the 21st century [147,148].

Nanoarchitectonics is a methodology for creating functional material systems by assembling nanounits such as atoms, molecules, and nano-objects (Figure 1) [149,150]. It can be thought of as architecture in the nano or material world. Methods of creating materials by assembling molecules and other materials have been also studied in supramolecular chemistry and other fields. Supramolecular assemblies have been formed through intermolecular interactions [151–155], inorganic mesoporous materials have been created through template synthesis [156–160], metal-organic frame work (MOF) with precise porous structures have been created through co-ordination chemistry [161–165], similar porous materials covalent organic framework (COF) can be constructed by polymer chemistry [166–170], and self-assembled monolayer (SAM) [171–175], Langmuir–Blodgett (LB) method [176–180], and layer-by-layer (LbL) assembly [181–185] have been developed with interface science. Although they have been successful, they are not unified and are rather independent. Nanoarchitectonics integrates these technologies into a unified field. Nanoarchitectonics is the broad integration of nanotechnology, including these material chemistry-related fields, various microfabrication technologies, biological processes, and so on. It must be

emphasized that rather than the creation of a new field, nanoarchitectonics is more of an integration of fields and a proposal for a unified concept.

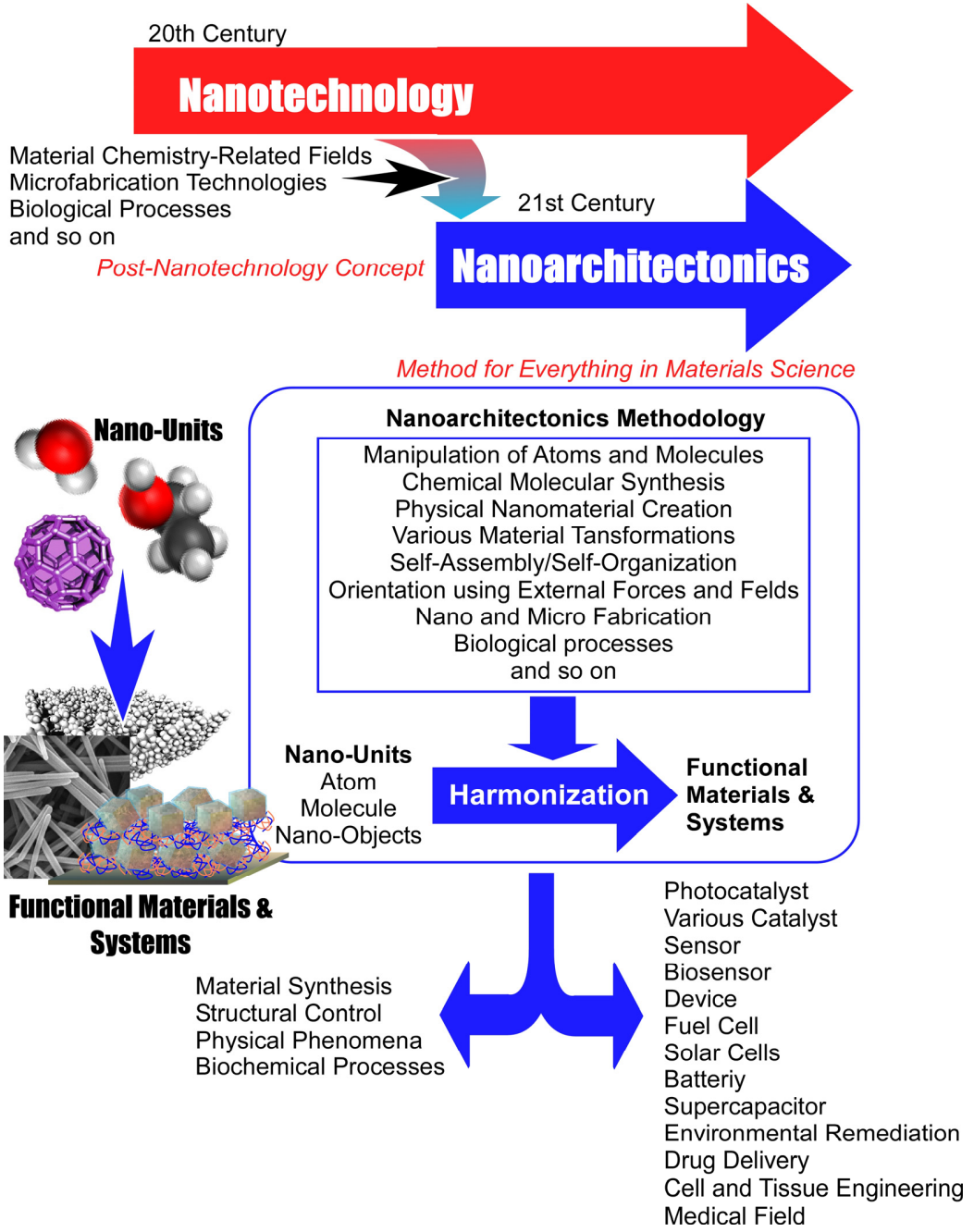

Figure 1. Outline, history, and effects of the nanoarchitectonics concept.

Therefore, material architecture through nanoarchitectonics will include a variety of elemental technologies: manipulation of atoms and molecules, chemical molecular synthesis, physical nanomaterial creation, various material transformations, self-assembly/self-organization, orientation using external forces and fields, nano and micro fabrication, biological processes, etc., in selected combinations, architecture of matter [186]. With these processes, materials construction often becomes multistep. Therefore, one of the characteristics of nanoarchitectonics is that it is easier to create hierarchical and asymmetric structures [187] than by simple self-assembly and other systems consisting of a single equilibrium [188]. In addition, phenomena in the nanoscale region are easily affected by various perturbations. For example, the effects of thermal fluctuations, stochastic distribu-

tions, and quantum effects might be involved. The approach of nanoarchitectonics is to harmonize the effects while balancing those ambiguities [189]. Hierarchical structures and the harmonization of several effects are similar to the characteristics of the organization of functional structures in biological systems. Nanoarchitectonics has the propensity to architect functional structures similar to those in biological systems [190,191]. In addition, the ultimate goal of nanoarchitectonics would be to create highly functional structures like those of living systems.

The above principles of nanoarchitectonics are very general. The target materials and their applications are not limited. The scientific papers advocating the term "nanoarchitectonics" cover a wide range of applications. It is used in basic areas such as material synthesis [192–198], structural control [199–205], the pursuit of physical phenomena [206–212], and basic biochemical processes [213–219]. Nanoarchitectonics is also widely applied in photocatalysts [220–226], various catalysts [227–233], sensors [234–240], biosensors [241–247], devices [248–254], fuel cells [255–261], solar cells [262–268], various batteries [269–275], supercapacitors [276–282], other energy systems [283–289], environmental remediation [290–296], drug delivery [297–303], cell and tissue engineering [304–310], and in medical fields [311–317]. Nanoarchitectonics is the concept of building functional material systems from atomic and molecular units. Because matter is originally composed of atoms and molecules, nanoarchitectonics can be a concept related to the creation of all matter. In physics, the ultimate physical principle is called "the theory of everything" [318]. Similarly, nanoarchitectonics can be a method for everything in materials science [319,320]. In fact, various materials development research projects that have not advocated nanoarchitectonics can be considered as nanoarchitectonics approaches under a broad concept.

Thus, the development of material science has culminated in the concept of nanoarchitectonics. However, the scope of application of nanoarchitectonics is wide, and it is somewhat difficult to encompass everything. Therefore, this review article will introduce the concepts of liquid and interface, which are keywords in the organization of functional material systems in biological systems, as mentioned above. At the interface, the movement and location of materials are restricted. In addition, phenomena unique to the interface also occur [321,322]. The interface is an attractive medium to develop nanoarchitectonics [323,324]. From this perspective, nanoarchitectonics for the LB method [325–327] and LbL assembly [328–331], which are interfacial processes, have been reviewed so far. In contrast, this review paper discusses nanoarchitectonics for interfaces in the liquid phase. The target interfaces are liquid–liquid interface, liquid–solid interface, and so on. As there are so many different examples falling under these fields, it is not necessarily appropriate to take an all-encompassing approach. A methodology that focuses on a few recent examples and extracts their characteristics is more practical. In this review paper, such cases are summarized under the categories of molecular assembly, MOF and COF, and living cell. In addition, the latest research on the liquid interfacial nanoarchitectonics of organic semiconductor film is also discussed. The final conclusive section summarizes these features and discusses what is needed for the development of liquid interfacial nanoarchitectonics and nanoarchitectonics in general.

2. Molecular Assembly

A liquid–liquid interface is a powerful site for the creation of nanostructures and materials from molecules. One such method is the liquid–liquid interfacial precipitation method [332]. This is a method to create structures by inducing molecular assembly at the interface created by immiscible solvents. The target molecule is dissolved in a good solvent, and a poor solvent is added to create a liquid–liquid interface. Then, due to the difference in solubility between the two solvents, insoluble aggregates or crystals of the target molecules are formed at the liquid–liquid interface. Depending on parameters such as the combination of solvents and the concentration of molecules in the good solvent, the structure and shape of the precipitated object will change. This is one method of nanoarchitectonics of materials from molecules. An interesting research example is the nanoarchitectonics of

fullerenes such as C_{60} and C_{70} at the liquid–liquid interface. Fullerenes are composed of only one element, carbon, and are essentially spherical in shape. They have no functional groups with which to interact. It is a simple entity: a single element and zero dimensionality. When such fullerenes are subjected to liquid–liquid interfacial precipitation, a wide variety of structures are obtained. This is a remarkable example of the diversity of nanoarchitectonics. One-dimensional nanowhiskers [333], nanorods [334], nanotubes [335], two-dimensional nanosheets [336,337], and three-dimensional nanocubes [338] are obtained by the liquid–liquid interfacial precipitation of fullerenes. These can be controlled simply by changing the combination of solvents, fullerene concentration, and mixing conditions. The diversity of structures can be further increased by coexisting or reacting compounds, or by post-treatment with solvents or different reagents. Complex and hierarchical structures can be obtained, such as rods extending from a cube [339], holes on each face of a cube [340], and holes in a cube like a gyrode [341], as well as structural changes analogous to biological differentiation and metamorphosis, such as the gradual growth of a tail from a spherical assembly [342]. From simple structures such as fullerenes, liquid–liquid interfacial nanoarchitectonics has the potential to produce a wide variety of structures with extremely simple manipulations.

Although the liquid–liquid interfacial precipitation strategy described above can be diversified by combining various components, the kinetic control process can further lead to a variety of morphological controls. Pursuant to this strategy, Chen et al. have successfully synthesized C_{60} spheres and their carbon materials of various sizes and morphologies by using droplets as templates (Figure 2) [343]. This method would allow for the mass production of solid or hollow C_{60} nanospheres with controlled sizes. The form in which the nanospheres are nanoarchitectonized is a matter of kinetically controlling the liquid–liquid interfacial precipitation process. This can be thought of as the kinetically controlled liquid–liquid interfacial precipitation (KC-LLIP) method. Specifically, 1,2-ethylenediamine was used as a covalent crosslinker for C_{60} molecules. It contributes to the in situ generation of ethylenediamine-C_{60} shells. The formation of ethylenediamine-C_{60} product was controlled by the addition of isopropyl alcohol. Sulfur was then added and the ethylenediamine-sulfur droplets were used as egg yolks. These droplets are important in creating a hollow structure via the formation of the yolk-shell structure. The nucleus of the 1,2-ethylenediamine-C_{60} complex adsorbs on the surface of the ethylenediamine-sulfur droplets. The former nuclei grow to form a shell of the ethylenediamine-C_{60} complex and the 1,2-ethylenediamine-sulfur droplets are removed by washing. As a result, hollow structures are obtained. The diversity of the C_{60} sphere structures produced is due to the regulation of the rate of structural growth of ethylenediamine-sulfur droplets and ethylenediamine-C_{60} complexes. Accordingly, the KC-LLIP method yields various forms of fullerene aggregates. The formations of porous spheres, string hollow spheres, hollow spheres, and open hollow spheres were observed. Because the morphology and dimensions of these C_{60} spheres can be tuned, they are expected to have a variety of applications. For example, they can be used as novel catalysts and catalyst supports. For this purpose, it is necessary to convert C_{60} aggregates into carbon materials using calcination treatment. Solid spheres, hollow spheres, and porous spheres were calcinized at 750 °C. Basically, they were carbonized while retaining their shape. High-resolution TEM suggested an amorphous carbon structure. Elemental mapping indicated a homogeneous distribution of carbon and nitrogen in these carbonized structures. The nitrogen-doped carbon sphere has an increased catalytic reaction surface due to the cavity structure. It is also a promising material as a catalyst and catalyst support because it prevents leakage of catalytic components. The exploration of such carbon nanomaterial synthesis strategies is crucial for the development of novel materials, as carbon spheres have a wide variety of potential applications in adsorbents, drug delivery, energy conversion and storage, and nanodevices, in addition to catalytic applications. The liquid–liquid interfacial nanoarchitectonics of kinetic control presented above could be a novel and groundbreaking approach. This simple process can yield carbon nanomaterials in a variety of forms, including size-defined solid spheres and hollow spheres with controllable pores and cavities. Based on this tactic, the advancement of nanoarchitectonics for the effective development of carbon materials for advanced applications is expected.

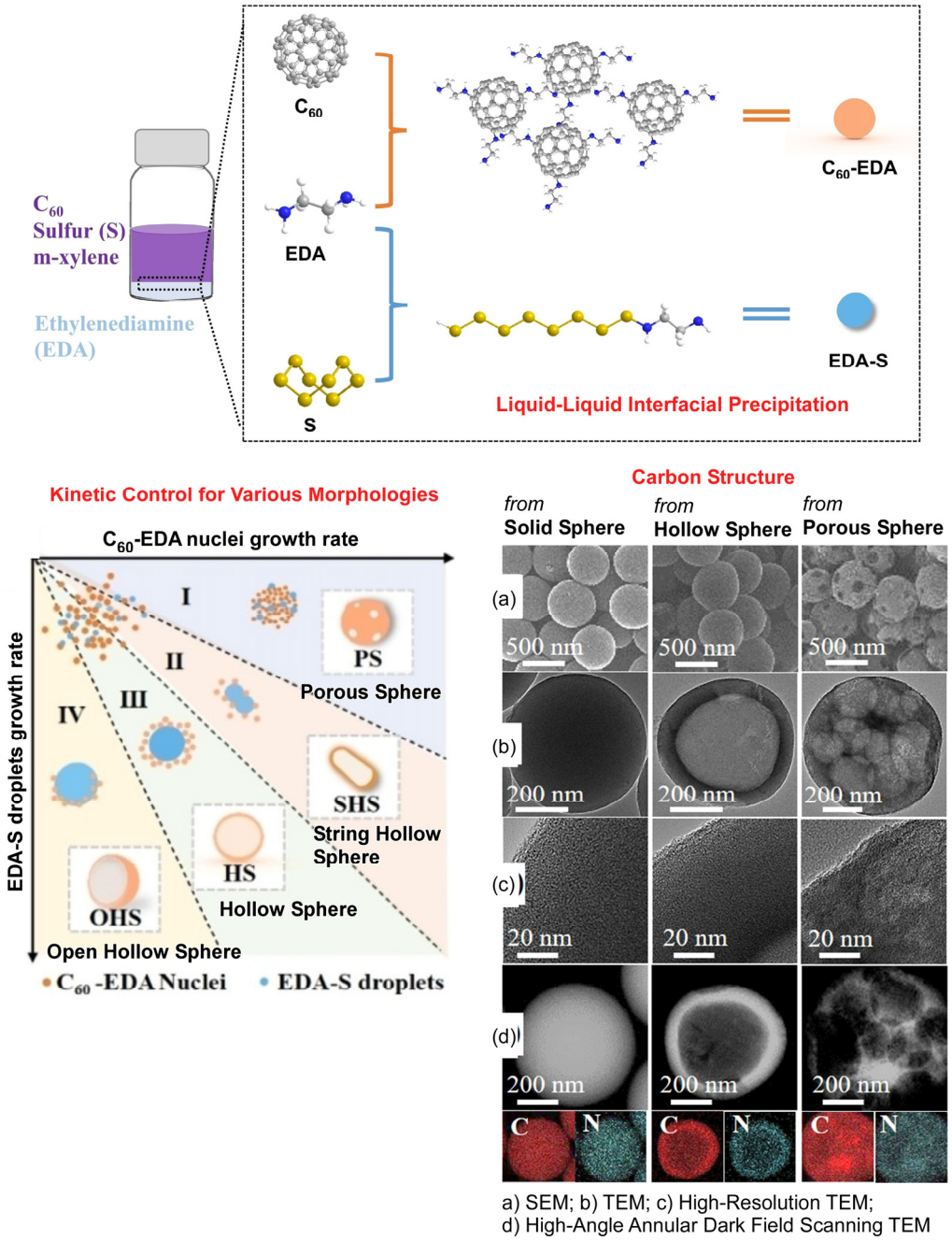

Figure 2. Kinetically controlled liquid–liquid interfacial precipitation (KC-LLIP) method to produce porous spheres, string hollow spheres, hollow spheres, and open hollow spheres from C_{60} with the aid of ethylenediamine and sulfur. The liquid–liquid interfacial precipitation method, kinetic control for various morphologies, and resulting carbon structures are explained. Reprinted with permission from [343]. Copyright 2022 Wiley-VCH.

Several studies have examined device properties of fullerene assemblies prepared by liquid–liquid interfacial nanoarchitectonics. Akiyama and co-workers prepared thin films of ethylenediamine-modified C_{60} nanoparticles and investigated their unique photochemical and electrochemical properties (Figure 3) [344]. The fluorescence and photocurrent generation properties of ITO electrodes modified with composite films with polythiophene were investigated. Ethylenediamine-C_{60} composite particles were prepared using liquid–liquid interfacial precipitation. A thin film of ethylenediamine-C_{60} composite microparticles was coated onto an ITO electrode modified with alternating adsorbed layers of

polyelectrolyte. In addition, polythiophene-modified, densely packed ethylenediamine-C_{60} particulate films were prepared using a combination of electrochemical polymerization of 2,2′-bithiophene. The fluorescent emission properties of the nanoarchitectonized composite films suggest that the ethylenediamine-C_{60}-adduct particulate film functions not only as an electron acceptor for polythiophene but also as a photosensitizer. The partial photocellular properties of electrodes composed of ethylenediamine-C_{60}-adduct particulate films and polythiophene were investigated. In the presence of methyl viologen, cathodic photocurrent was generated by excitation of the composite films. The obtained results suggest various possibilities of composite thin films of ethylenediamine-C_{60}-adduct particulate films and polythiophene. In particular, the possibility of application to photoelectrochemical devices such as photoelectric conversion devices and sensors is promising.

Because liquid–liquid interfacial nanoarchitectonics is a powerful tool for structuring functional molecules other than fullerenes, Takase, Shimizu, and co-workers have prepared a highly conductive charge-transfer complex, (phthalocyaninato)cobalt iodide, at the liquid interface [345]. It is very important to make cobalt phthalocyanine industrially practical as a catalyst for CO_2 reduction. For this purpose, it is necessary to study the influence of the conductivity enhancement of cobalt phthalocyanine crystals on the catalytic activity. From this perspective, a highly conductive charge-transfer complex, (phthalocyaninato)cobalt iodide, was investigated. In this approach, (phthalocyaninato)cobalt iodide is easily assembled by simply mixing a KI solution containing trifluoroacetic acid and cobalt phthalocyanine with a CH_2Cl_2 solution at the interface, applying the cobalt phthalocyanine crystal phase transition method. Moreover, UV–Vis analysis showed that I^- is changed to $I_3{}^-$ at the interface. The resulting material consists of a one-dimensional column of cobalt phthalocyanine and a linear array of $I_3{}^-$. The catalytic properties of (phthalocyaninato)cobalt iodide were investigated using polarization measurements and electrochemical impedance spectroscopy using a gas diffusion carbon electrode. The results showed high catalytic activity for CO_2 reduction. In addition, high CO formation selectivity was obtained. This liquid–liquid interfacial nanoarchitectonics method has the potential to yield a variety of charge transfer complexes with $I_3{}^-$. Such nanoarchitectonized materials are expected to be applied to electrochemical devices.

Nanoemulsion provides a microscopic liquid–liquid interface. This environment is also an excellent environment in which to develop molecular nanoarchitectonics. However, for therapeutic and diagnostic applications of nanoemulsions, it is necessary to introduce appropriate functional groups at the interface. In particular, it is essential to develop methods for modifying liquid–liquid (oil–water) interfaces stabilized by surfactants. Modification techniques using lipophilic nitrile N-oxide compounds were developed by Niko and coworkers (Figure 4) [346]. The lipophilic nitrile N-oxide compounds are highly soluble in oil. Therefore, they can be easily introduced into the interface of nanoemulsions. The lipophilic nitrile N-oxide compounds introduced at the oil–water interface reacted efficiently with functional molecules having C=C or C≡C bonds at the ends under catalyst-free conditions. This is a 1,3-dipolar cycloaddition reaction. Surface-functionalized nanoemulsions can be used without any distinctive purification. Nanoemulsions containing lipophilic cyanine 3.5, a fluorescent dye molecule, and lipophilic nitrile N-oxide compounds were used for nanoarchitectonics. They were further functionalized with pheophorbide a, a photosensitizer that generates singlet oxygen for photodynamic therapy. This modification was confirmed by Förster resonance energy transfer analysis. When the lipophilic cyanine 3.5 molecules in the nanoemulsions were photoexcited, the excitation energy was efficiently transferred to pheophorbide a via Förster resonance energy transfer. These nanoemulsions can function as light-focusing nanoantennae. Therefore, this nanoemulsion system showed 7–18 times more efficient singlet oxygen generation than direct excitation of pheophorbide a. It was confirmed that despite the reduced cell permeability, efficient singlet oxygen generation induces cancer cell death. Surface modification techniques based on lipophilic nitrile N-oxide compounds are expected to be both practically useful and promising. The development of theragnostic materials based on nanoemulsions for selective tumor targeting, for example,

is expected. Furthermore, this interfacial nanoarchitectonics approach could be applied to surface modification of other types of nanomaterials, such as polymeric nanoassemblies, micelles, and liposomes. In turn, it can be a promising method for imparting various functional groups and functions to bionanomaterials.

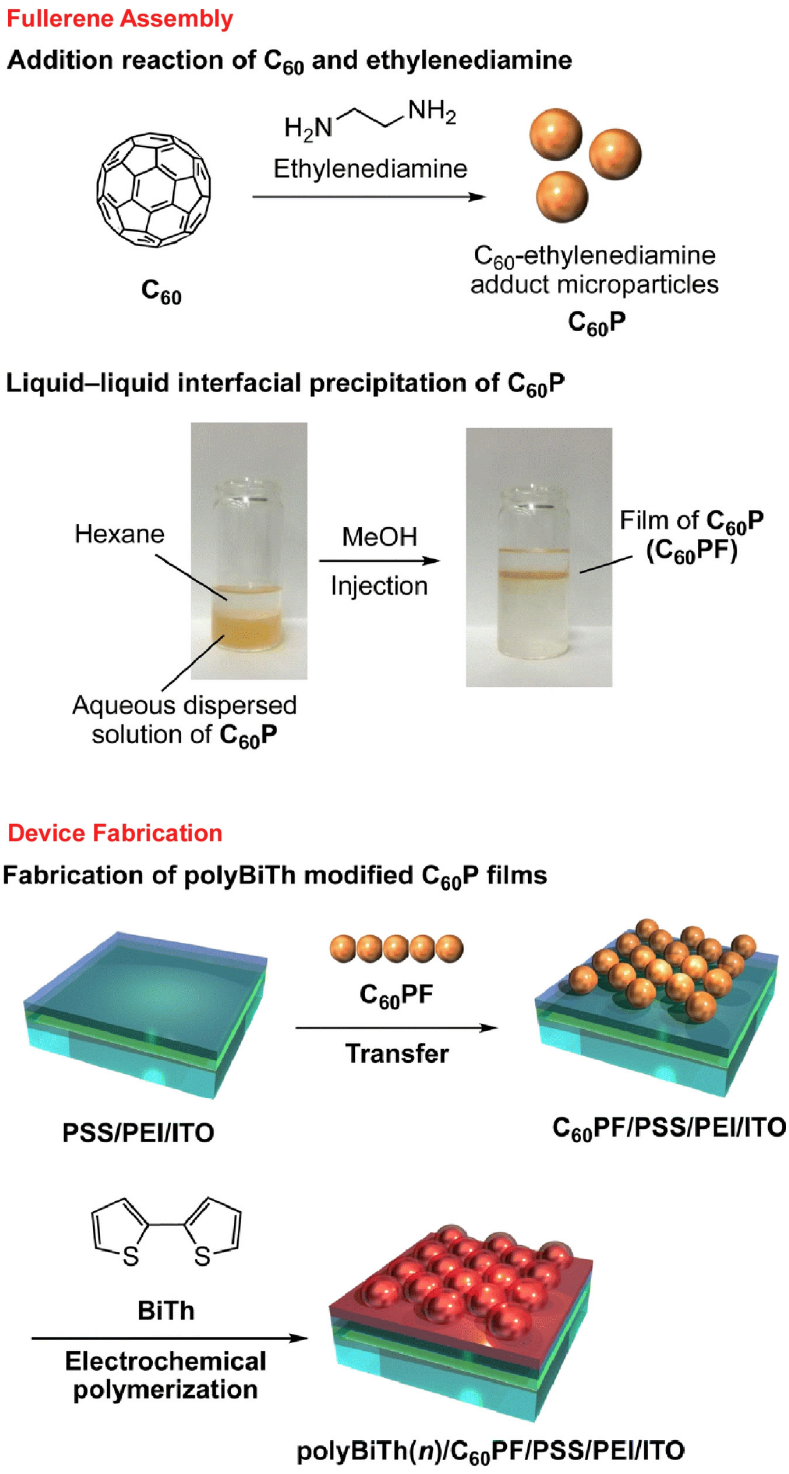

Figure 3. Preparation of thin films of ethylenediamine-modified C_{60} nanoparticles on an ITO electrode modified with alternating adsorbed layers of polyelectrolyte for a device with their unique photochemical and electrochemical properties. Fullerene assembly (**top**) and device preparation (**bottom**) are explained. Reproduced under terms of the CC-BY license [344]. Copyright 2023 Royal Society of Chemistry.

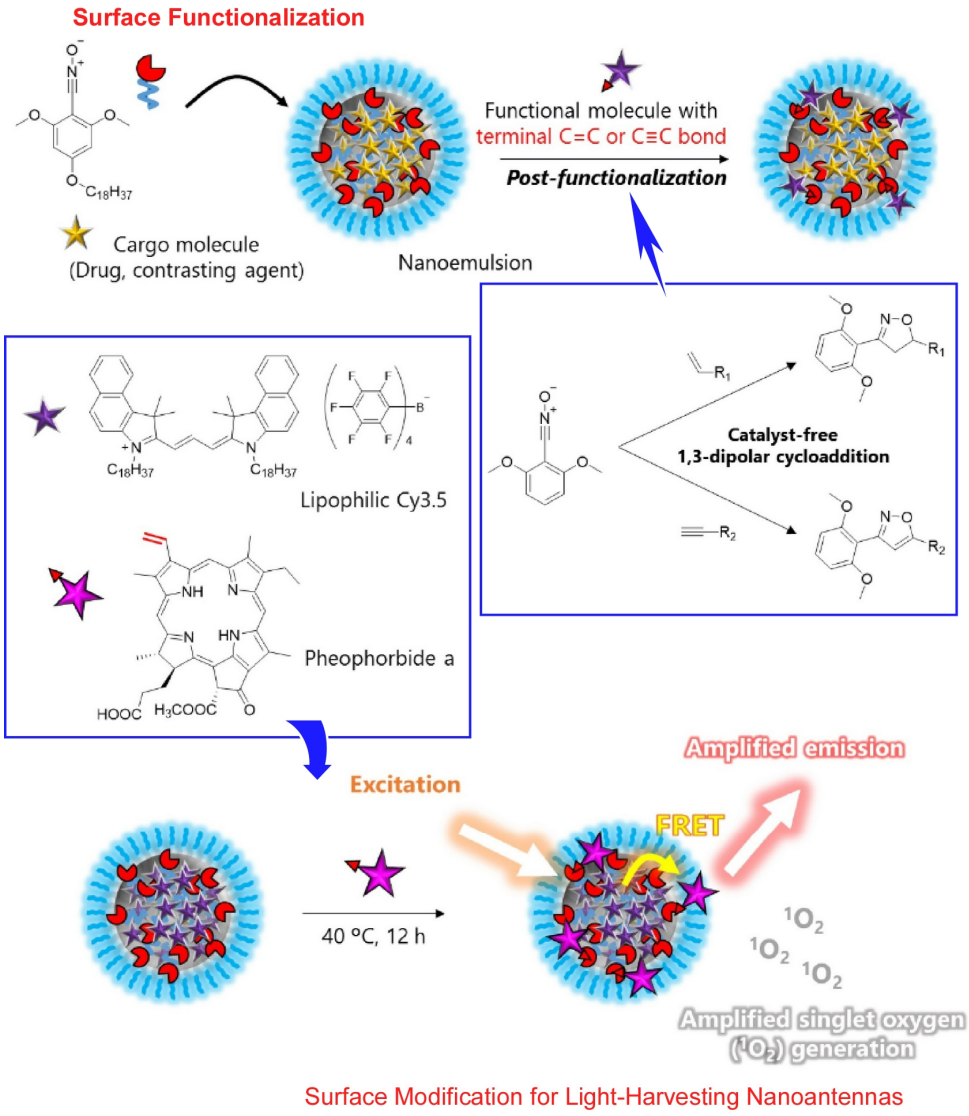

Figure 4. Introduction of lipophilic nitrile N-oxide compound for surface-functionalized nanoemulsions containing lipophilic cyanine 3.5 and a fluorescent dye molecule, where further functionalization with pheophorbide a, as a photosensitizer, generates singlet oxygen for photodynamic therapy. Surface functionalization (**top**) and surface modification for light-harvesting nanoantennae (**bottom**) are explained. Reprinted with permission from [346]. Copyright 2023 Oxford University Press.

3. MOF and COF

This section focuses on metal-organic frameworks (MOFs) [347–351] and covalent-organic frameworks (COFs) [352–356] as targets for liquid interfacial nanoarchitectonics. Nanoporous materials have been actively studied from the viewpoint of various applications, and MOFs and COFs are representative categories. MOFs build up regular porous structures through co-ordination chemistry, whereas COFs do so through polymer chemistry. Both approaches are typical of nanoarchitectonics, which builds functional structures from building blocks. They are often prepared as two-dimensional structures at liquid interfaces [357–359]. MOF and COF can be representative players in liquid interfacial nanoarchitectonics.

In particular, these structures hold much promise from an application standpoint. MOFs have a large surface area and can store a large amount of photogenerated charge on their surface sites. Applications in photoelectrochemical capacitors are being considered. Photoelectrochemical capacitors have attracted attention for their charge accumulation and dissipation mechanisms, as well as for their spike and overshoot current properties.

These properties are of interest for biomedical applications such as optical stimulation of nerves and sensing of biomolecules, etc. Moribe et al. have conducted a fundamental exploration into the application of MOFs to photoelectrochemical capacitors [360]. Transient photocurrent measurements were performed in a photoelectrochemical capacitor cell consisting of a porphyrin zirconium MOF electrode at the liquid–solid interface of phosphate-buffered saline and an electrode. In transient photoelectrochemical capacitor cell transient photocurrent measurements using MOF electrodes in phosphate buffer solution under an argon atmosphere, spike and overshoot photocurrents were observed. A clear growth and decay of cathodic current was observed during light irradiation. When the light was turned off, an anodic reverse current was generated, inducing spike and overshoot currents. The direction of the induced current indicated that the MOF electrode behaved like a p-type photoelectrochemical capacitor cell electrode. No spike or overshoot currents were observed when excess oxygen was introduced into the electrolyte. The obtained results suggest that the porphyrin zirconium MOF electrode accumulates charge at the surface site in the MOF pore closest to the electrolyte–electrode interface, which is the liquid–solid interface. Thus, porphyrin zirconium MOFs are expected to be promising for biomedical applications as photoelectrochemical capacitors. This is because quantitative sensing of biological phenomena, such as those seen in the photostimulation of neurons, may be possible. This has potential for future biomedical applications. Investigation and improvement of the stability of the MOF electrode in the biological environment is also very important for its practical application.

COF is also used for a variety of applications, including various devices. For example, the construction of uniform COF films on electronic device substrates is a desirable technique to be established. Chen and co-workers have developed a method to prepare COF films by polymerization at the liquid–solid interface under simple and mild conditions (Figure 5) [361]. They demonstrate the mild synthesis of five different highly crystalline two-dimensional COFs at room temperature using amino and aldehyde precursors with different geometric configurations. The resulting COF films have a large lateral size, controllable thickness, and high crystallinity. In addition, they are uniform and free of contamination, wrinkles, and damage when viewed under an optical microscope. Furthermore, they could be formed directly on the device substrate by interface engineering. The latter property is particularly advantageous for the fabrication of device arrays. For example, molecular dynamics simulations have shown that the presence of –OH groups on the solid surfaces strengthens the interaction energy between the substrate surface and the precursor. Promoting adsorption of precursors is advantageous for thin film fabrication. In other words, by selectively treating the substrate, pattern growth of COF films can be achieved. Furthermore, the COF films exhibit excellent chemical stability in DMF, MeOH, THF, H_2O, NaOH, and HCl solutions and can withstand temperatures as high as 450 °C. COF films have high crystallinity and photoelectrochemical performance. The excellent stability is also beneficial for photoelectrochemical applications. 4,4′,4′,4′-(1,3,6,8-tetrakis(4-aminophenyl)pyrene and terephthalaldehyde. When used as active materials in electronic devices, they showed efficient responses. The obtained results are comparable to those of several metal-containing inorganic and carbon materials. When used as an active material in synaptic devices, excellent synaptic plasticity properties were obtained with light stimulation. Biological synaptic functions, such as short-term plasticity, long-term plasticity, and conversion from short-term to long-term plasticity, as well as superior synaptic plasticity properties induced by light stimulation, were successfully simulated. The liquid interfacial nanoarchitectonics method developed in this study will also lead to the large-scale facilitated preparation of COF membranes. It is expected to pave the way for multifunctional applications in optoelectronics, demonstrating their functionality.

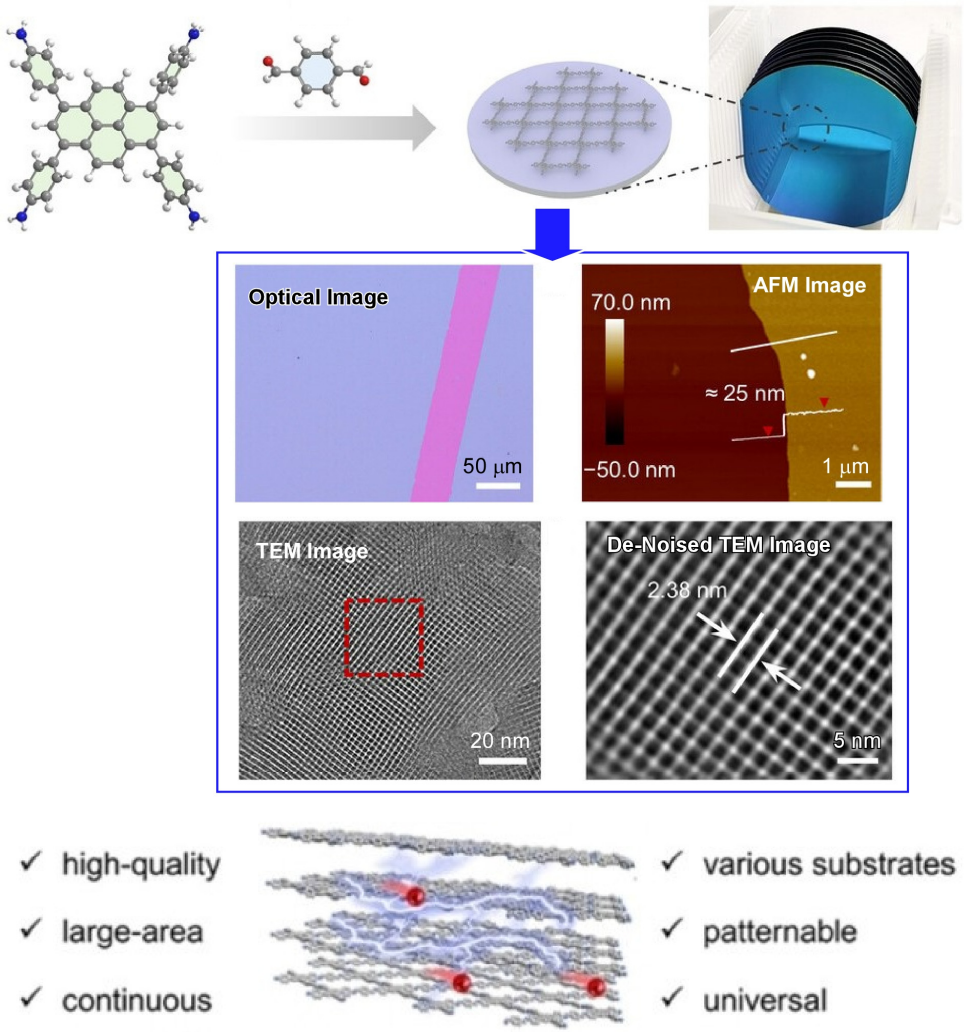

Figure 5. Preparation of COF films by polymerization at the liquid–solid interface under simple and mild conditions to result in various good features of a large lateral size, controllable thickness, high crystallinity, uniformity, and being free of contamination, wrinkles, and damage. Fabrication method (**top**), images (**middle**), and typical features (**bottom**) are explained. Reprinted with permission from [361]. Copyright 2024 Wiley-VCH.

An advanced reaction system of interest is the Pickering emulsion stabilized by solid particles. Such Pickering emulsions increase the oil–water interface and the liquid–liquid interface. As a result, they promote two-phase catalytic reactions. At the emulsion–liquid interface, the microenvironment and nanospatial properties of the reaction are controlled. Accordingly, reaction selectivity can be controlled. The compartmentalized droplet geometry can also be used to process continuous flow catalytic reactions. The use of advanced amphiphilic solid catalysts is essential for the development of superior Pickering emulsion catalysts. To form stable Pickering emulsions, substances adsorbing at the oil–water interface need to have appropriate amphiphilicity. Liquid interfacial nanoarchitectonics of such substances is desired. Zou, Fang, and co-workers showed that COF nanoparticles synthesized with highly hydrophobic monomers as linkers have excellent amphiphilic properties [362]. Furthermore, they showed that this COF structure is useful for Pickering emulsification catalysts (Figure 6). The amphiphilic COFs developed here can be used as solid emulsifiers to control emulsion type and droplet size. More importantly, the particle size of these COF nanoparticles is highly controllable. In other words, with high surface area and tunable pore diameter, catalytic systems with high reaction efficiency and excellent size selectivity can be achieved. For proof of concept, alcohol oxidation under two-phase

conditions was investigated. For this purpose, Pd nanoparticles were encapsulated within these amphiphilic COF nanoparticles. The nanoarchitectonically prepared catalyst exhibited a catalytic efficiency that was 3.9 times higher than that of conventional amphiphilic solid catalysts. The significant increase in catalytic activity is still attributed to the high surface area and regular porous structure of the COFs. The nanoarchitectonics of the COFs is thought to be responsible for the assembly of fast channels that facilitate mass transfer at the Pickering droplet interface. The construction of COF structures by liquid interfacial nanoarchitectonics is expected to provide an innovative platform for Pickering emulsification catalysis.

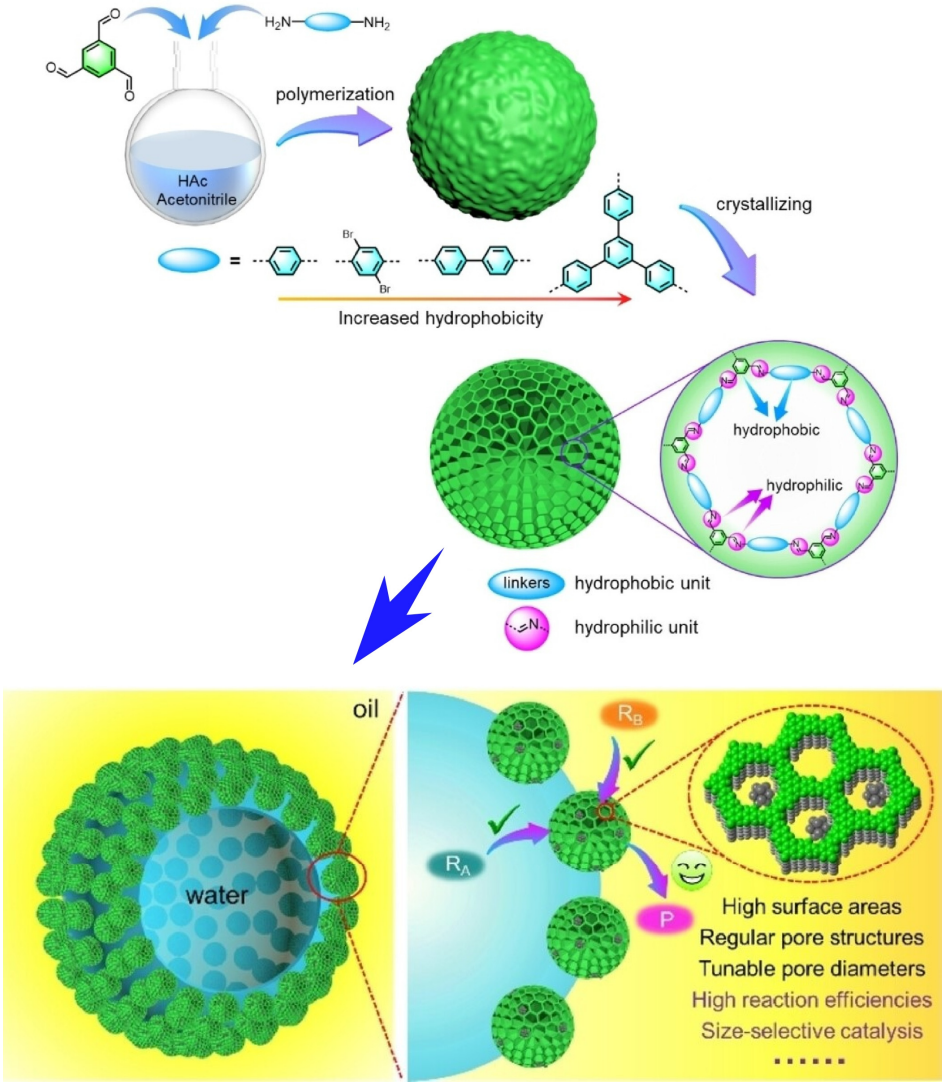

Figure 6. Preparation of COF structure on Pickering emulsion as controllable catalysts with a high surface area and tunable pore diameter to provide high reaction efficiency and excellent size selectivity. Structure fabrication method (**top**) and properties and functions (**bottom**) are explained. Reprinted with permission from [362]. Copyright 2024 Wiley-VCH.

Highly flexible and robust self-assembled COF membranes are used in a variety of applications. An example is their application as precision separation membranes. However, the synthesis of stable and functional COF membranes that actually exhibit useful functions is, surprisingly, technically challenging. Liu and co-workers synthesized a two-dimensional soft COF (SCOF) based on an imine structure using a flexible linker of aldehydes and triangular building blocks (Figure 7) [363]. This technique yields very large-area (two-dimensional and soft) COF molecular membranes. The synthesis uses a

liquid–liquid interface consisting of water/dichloromethane as the reaction field. Rigid tris(4-aminophenyl)amine and flexible glutaraldehyde monomer are used as building blocks for the two-dimensional COF membrane. Sodium dodecyl sulfate is oriented at this liquid interface, and structures such as molecular crosslinks are self-assembled. The sodium dodecyl sulfate molecules facilitate the migration of tris(4-aminophenyl)amine, making the contact between the amine and aldehyde monomers faster and more homogeneous. This led to a record-breaking rate of preparation of the COF membranes and the appearance of more uniform pores. The nanoarchitectonically prepared two-dimensional COF membranes showed excellent sieving ability for small molecules. They were also resistant to strong alkalis (5 M NaOH), acids (0.1 M HCl), and various organic solutions. It also had the necessary flexibility as a membrane for practical use. The porous two-dimensional COF membranes are easy to fabricate and the pore size can be adjusted. As a result, they have the functional property of allowing precise molecular sieving. This nanoarchitectonics of the separation membrane was programmed from building blocks at the molecular level. The structures created have great potential for trace contaminant removal, drug/organic solution separation, oil/water separation, metal ion screening, alcohol/water separation, gas separation, and chiral discriminations.

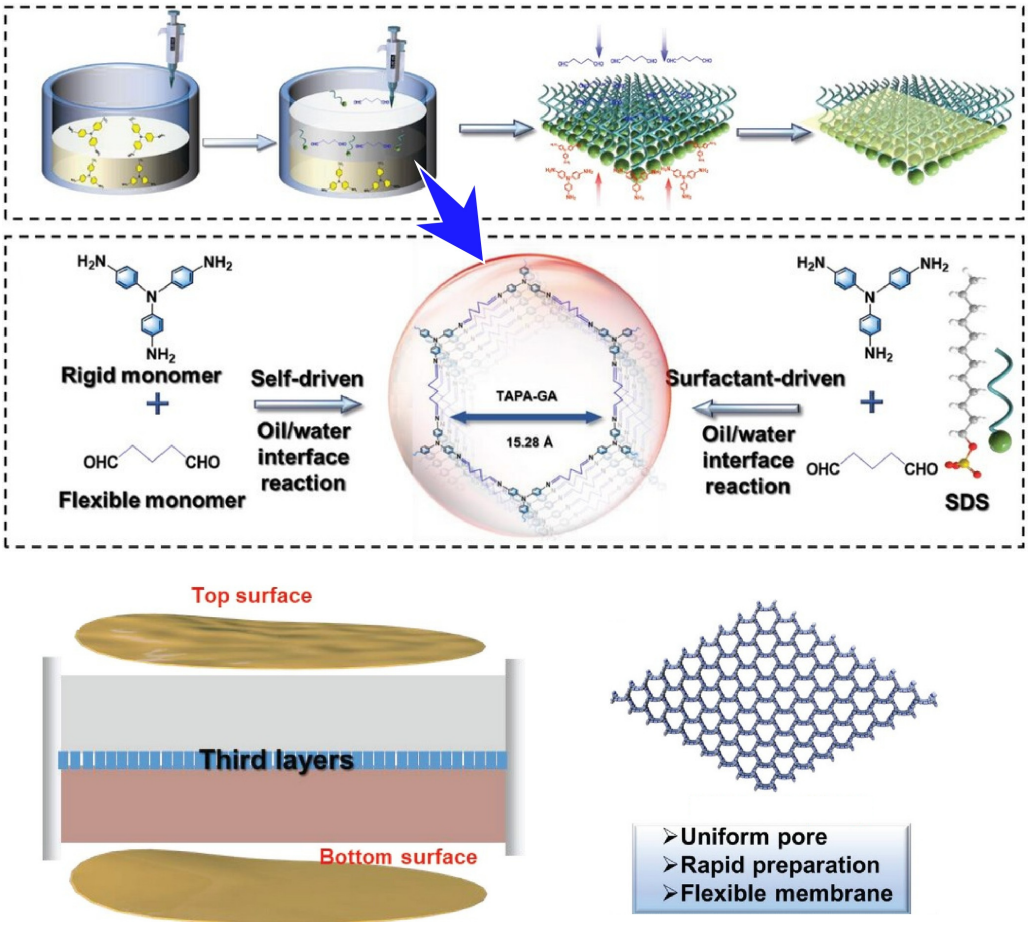

Figure 7. Synthesis of a two-dimensional soft COF (SCOF) based on an imine structure using a flex-ible linker of aldehydes and triangular building blocks, where sodium dodecyl sulfate molecules facilitate the migration of tris(4-aminophenyl)amine, making the contact between the amine and aldehyde monomers faster and more homogeneous. Reprinted with permission from [363]. Copyright 2023 Wiley-VCH.

4. Living Cell

Liquid interfaces can also contribute to a variety of biotechnology-related controls. One of the more complex systems is the control of cell culture and associated cell differentiation.

In other words, nanoarchitectonics can be applied even at the living cell level of complexity. Cell culture is usually carried out at the interface between liquid and solid, such as the interface between solid surfaces and culture medium. The cells detect the mechanical properties of the solid interface, which in turn control their behavior and function [364–366]. This area of research is also being developed as mechanobiology [367–369]. Recently, pioneering systems that do not use solid interfaces have been reported. The interface between immiscible liquids is used as a culture environment for cells. In particular, organic solvents, such as perfluorocarbons, which do not adversely affect cells, are used as organic solvent layers [370]. It is now known that structures such as protein molecular membranes can be spontaneously nanoarchitectonized at such a liquid–liquid interface and influence cell differentiation [371]. Cells are influenced by the environment with which they come into contact to alter their behavior and function. It has been known that static properties such as the stiffness, nanotopography, and geometry of the materials with which cells come in contact have a significant impact. In addition, the viscoelastic properties of the matrix with stress relaxation are important in controlling cell fate and activity.

As an example, stem cells interact with the extracellular matrix and remodel it, which determines the fate of stem cells. The liquid–liquid interface, which is unaffected by the solid substrate, can be an ideal environmental site in which to explore the nature of cell behaviors. Jia et al. studied the effect of a two-dimensional network of protein nanofibrils spontaneously formed at the liquid–liquid interface composed of aqueous culture medium and fluorocarbons on stem cell behaviors (Figure 8) [372]. In particular, it was found that lipid raft formation and phosphorylation of focal adhesion kinase affect stem cell differentiation at the liquid–liquid interface. Protein nanofibrils are on the order of several microns in length and are in a form of polymeric β-sheet aggregates of proteins. They are biocompatible for cell adhesion and have high mechanical strength, which can mimic natural extracellular matrix fibers. Culturing stem cells on a two-dimensional network of protein nanofibrils at the liquid–liquid interface of water–perfluorocarbon promoted neural differentiation. In this process, lipid raft microdomains play a central role in both the initial cell adhesion and neural differentiation of stem cells. Lipid rafts help contact the cell membrane by containing cell adhesion molecules and provide a site for the enrichment of functional sites. They aid in the formation of large signaling complexes. As a result, stem cells are able to rapidly adapt to their constantly changing microenvironment. They integrate downstream signals involving focal adhesion kinase in lipid rafts within membrane microdomains. As a result, neurogenesis of stem cells is induced. The example shown here is just one example. The nanoarchitectonics of liquid interfaces incorporating bioactive proteins and responsive polymers will likely find applications in regenerative medicine and tissue engineering. Liquid–liquid interfaces can contribute to the development of nanoarchitectonics for previously unimagined adaptive biomaterials.

As illustrated in the examples above, cells also exhibit mechanosensing behavior at the liquid–liquid interface. Cell adhesion at the liquid–liquid interface is often mediated by the protein nanolayers derived from the culture medium that form at the interface. The media that form the liquid–liquid interface are not limited to the phase-separated structures of water and perfluorocarbons. Ueki et al. have developed a liquid–liquid interface culture technique using hydrophobic ionic liquids as the water-immiscible phase [373]. The diversity of ionic liquids is wide. By changing the chemical structure of the components or the combination of ions, their properties can vary greatly. The range of physicochemical parameters such as polarity, viscosity, surface tension, and ionic properties can be greatly varied. From this perspective, ionic liquids are often referred to as designer solvents. Their advantage over perfluorocarbons is their high solubility in a wide variety of substances. This allows for adaptation of cell control at the liquid–liquid interface. From among the diverse options, alkylphosphonium-type ionic liquids were found to be promising as ionic liquids with negligible cytotoxicity. The van der Waals interactions of the constituent ions and the charge distribution of the cations were investigated in terms of protein nanolayer formation and cell adhesion behavior mediating cell culture. Such studies could be applied

to emulsion systems with a wide range of liquid–liquid interfaces. Emulsion with cell culture medium as the continuous phase and hydrophobic liquid as the dispersed phase could be a cell culture method that does not require plastic dishes. Cell resources can be recovered by using a filtration process that does not require trypsin enzyme treatment, facilitating full automation of the cell culture process.

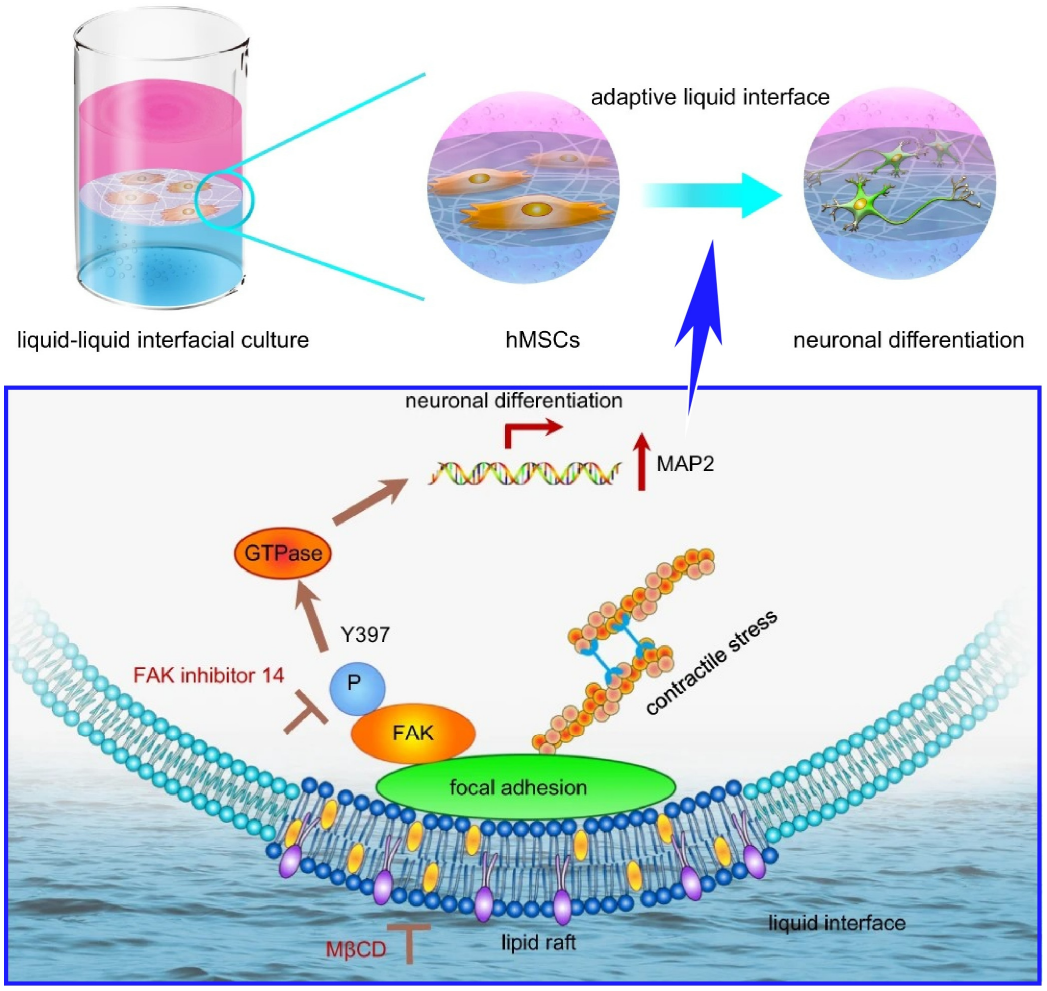

Figure 8. Effect of a two-dimensional network of protein nanofibrils spontaneously formed at the liquid–liquid interface composed of aqueous culture medium and fluorocarbons on stem cell behaviors, where lipid raft microdomains play a central role in both the initial cell adhesion and neural differentiation of stem cells through the integration of downstream signals involving focal adhesion kinase. Reproduced under terms of the CC-BY license [372]. Copyright 2022 Springer-Nature.

As a cell culture at the liquid–liquid interface, cell culture on micro-oil droplet surfaces is an environmentally benign alternative compared plastic dishes, which are implicated in the generation of microplastics. In addition, it is a strategy that can scale up the production of adherent cells by increasing the size of the system. The presence of proteins that function at the liquid interface is essential for cell culture on such micro-oil droplet surfaces. Gautrot and co-workers have developed a new class of protein nanosheets that serve these purposes by co-assembling supercharged albumin with a pentafluorobenzoyl chloride surfactant (Figure 9) [374]. It was found that the protein nanosheets formed by the liquid interfacial nanoarchitectonics mediate the adsorption of extracellular matrix proteins and cell adhesion. The behavior of the protein nanosheets was quantified by surface plasmon resonance and fluorescence microscopy. Supercharged albumin retains tension-active properties suitable for stabilizing microdroplets. Coupling with pentafluorobenzoyl chloride surfactant results in strong interfacial elastic properties. The protein nanosheet formed plays a dual role. It

serves as a scaffold protein that structures the liquid–liquid interface and as a substrate for trapping extracellular matrix molecules. The adhesion and proliferation of human epidermal stem cells in bioemulsions stabilized by pinned droplets and supercharged nanosheets were also investigated. The methodology presented in this study results in a system that does not require plastics. It has the potential to revolutionize the cell manufacturing process and address environmental problems.

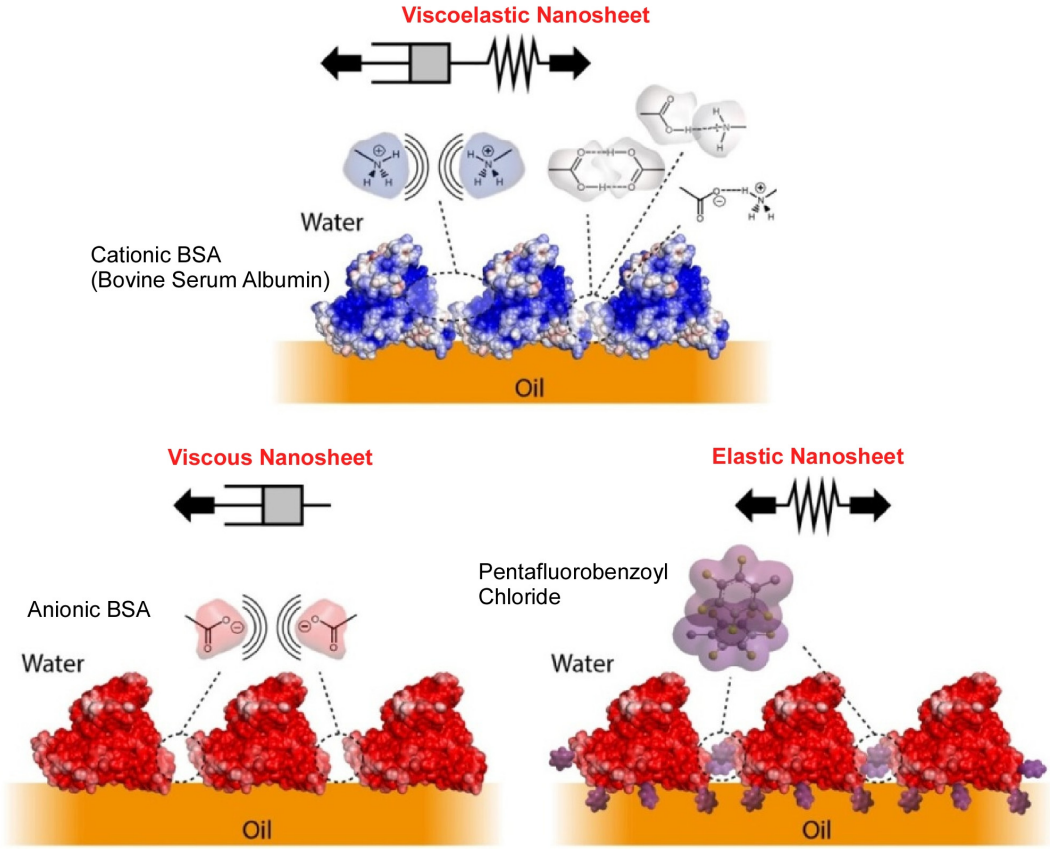

Figure 9. Protein nanosheets formed by co-assembling super-charged albumin with a pentafluorobenzoyl chloride surfactant, where coupling with pentafluorobenzoyl chloride surfactant results in strong interfacial elastic properties. Viscoelastic nanosheet (**top**), viscous nanosheet (**bottom left**), and elastic nanosheet (**bottom right**) are exemplified. Reproduced under terms of the CC-BY license [372]. Copyright 2023 American Chemical Society.

As discussed above, bioemulsions provide a promising venue for the growth of adherent cells in bioreactors. Their functionality depends on the development of protein nanosheets that are nanoarchitectonized at the liquid–liquid interface. Factors such as suitable interfacial mechanical properties and the promotion of integrin-mediated cell adhesion are important. Gautrot and co-workers investigated the effect of aliphatic surfactants such as palmitoyl chloride and sebacoyl chloride on the nanosheets formed by poly(L-lysine) at the liquid interface [375]. The assembly kinetics, interfacial shear dynamics, and viscoelasticity of poly(L-lysine) at the silicone oil interface were investigated. Using immunostaining and fluorescence microscopy, the effect of poly(L-lysine) nanosheets on mesenchymal stem cell adhesion was examined. The results revealed that the classical focal adhesion-actin cytoskeleton mechanism is involved. The proliferation of mesenchymal stem cells at the interface of other non-fluorinated oils, based on mineral and vegetable oils, was also investigated. Mesenchymal stem cells also developed focal adhesion at the silicone oil interface stabilized with poly(L-lysine) nanosheets. In doing so, they formed a mature actin cytoskeleton. Successful cell culture at non-fluorinated bioemulsion interfaces and systematic characterization of cellular phenotypes are also expected. Valuable insights

were gained toward the realization of stem cell culture on mineral and plant-derived oil surfaces relevant to the healthcare and cultured meat industry. There are also many advantages from an engineering perspective. For example, simply centrifuging or filtering the cultures would facilitate the recovery of cellular products from the bioemulsion and subsequent processes.

5. Frontier Research, Organic Semiconductor

As the final example of liquid interface nanoarchitectonics, doping of organic semiconductors at the liquid–solid interface is described in this section. In semiconductor science and industry, inorganic semiconductors have taken the lead [376–378]. The development of the semiconductor industry is also an important part of national strategy. Therefore, technologies related to inorganic semiconductors have developed ahead of their time. On the other hand, it is said that technological development is approaching its limits. As an alternative, the development of organic semiconductor technology is desired [379–381]. The advantage of organic semiconductors is that they are easy to process, cheap, and can be mass produced. Another advantage is that flexible devices can be made. Electronic devices can be produced by low-cost printing such as inkjet printing. For this reason, their use in various flexible devices such as film sensors, electronic circuits, solar cells, light-emitting diodes, displays, and biological sensing devices are being studied worldwide. On the other hand, they are far inferior to inorganic semiconductors in terms of electrical conductivity and other properties. Therefore, the process of doping, which controls the ease of electricity flow in semiconductors, is essential for organic semiconductor materials [382–384]. For example, doping in organic semiconductors has been performed by chemical doping using reactions with redox reagents. However, redox reagents are easily degraded by reactions with water in the air. Therefore, chemical doping often requires special facilities to handle reagents in a vacuum or nitrogen atmosphere. In addition, problems have arisen regarding the accuracy and reproducibility of chemical doping due to the instability of redox reagents. These are major barriers to the fabrication of flexible devices and industrial applications using organic semiconductors. Innovative advances in doping technology for organic semiconductor thin films need to be made through liquid interfacial nanoarchitectonics.

With this background, Ishii, Yamashita, and co-workers developed a chemical doping process controlled by proton activity in water (Figure 10) [385]. Chemical doping is based on electron transfer reactions between molecular semiconductors and dopant molecules. In this case, the redox potential of the dopant is the key to controlling the Fermi level of the semiconductor. In this new method, doping conjugated with proton coupling electron transfer reaction is proposed. The synergistic reaction between proton coupling electron transfer reaction and ion intercalation has led to efficient chemical doping of crystalline organic semiconductor thin films under room temperature conditions. Polymeric organic semiconductor thin films were immersed in an aqueous solution containing a benzoquinone/hydroquinone system and hydrophobic molecular ions. When conversing from benzoquinone to hydroquinone, electrons are taken from the organic semiconductor, and holes are injected into the organic semiconductor at that time. At the same time, hole injection is stabilized by intercalation of hydrophobic ions. As the equilibrium between benzoquinone and hydroquinone is determined by the pH in the aqueous solution, the number of holes injected is precisely determined by the pH of the aqueous solution. The process is reproducible under normal temperature conditions in this pH-controlled aqueous solution. It shows unprecedented scalability, stability, and tunability. Chemical doping requires no special equipment for handling reagents in a vacuum or nitrogen atmosphere. This technology, which allows precise control of doping levels, is also expected to lead to the development of innovative sensors. Thin-film organic semiconductor sensors that measure pH and ion concentrations are expected to contribute to healthcare and biosensing technologies. Thus, the coupling of the nanoarchitectonics of liquid interfaces with chemical equilibrium and doping phenomena could bring innovation to the semiconductor industry.

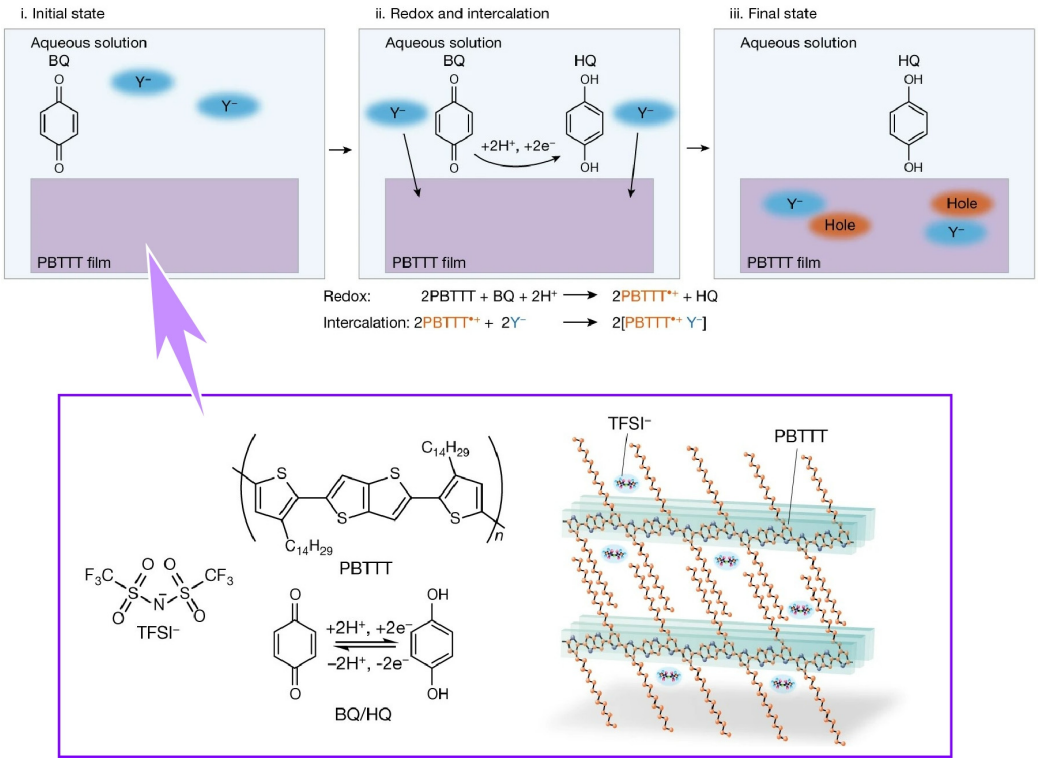

Figure 10. The synergistic reaction between proton coupling electron transfer reaction and ion intercalation leading to efficient chemical doping of crystalline organic semiconductor thin films under room temperature conditions. The doping mechanism (**top**) and chemical structure (**bottom**) are exemplified. Reprinted with permission from [385]. Copyright 2023 Springer-Nature.

6. Summary and Perspectives

In this paper, a brief description of nanoarchitectonics, which is a forefront concept in the development of artificial materials, is given. It then presented several recent examples that focused on the field of the liquid interface. Examples of the contributions of liquid interfacial nanoarchitectonics are as diverse as the examples given here. Examples include the creation of molecular complexes and assemblies, the construction of nano-regular structures such as MOFs and COFs, the control of living cells, and innovative doping techniques for organic semiconductors.

The diversity is due to the variety of elements that make up the liquid–liquid interface. In the case of liquid–liquid interfacial nanoarchitectonics, a variety of substances can be created that meet and form at the interface, depending on the components to be dissolved in each layer. Even simple molecules such as fullerenes can be nanoarchitectonically assembled in a variety of ways, depending on the choice of solvent and conditions. The resulting possibilities are endless. Until now, such approaches have been supported by simple mechanisms and the experience of researchers. Artificial intelligence (AI) will need to be introduced in order to make greater progress. Machine learning is being actively used to optimize the synthesis of materials and to elucidate the chemical phenomena that form the basis of such synthesis [386–390]. The need to integrate nanoarchitectonics and materials informatics is also being discussed [391,392]. Liquid interfacial nanoarchitectonics, with its diverse possibilities, is considered to be a very meaningful subject for the introduction of AI.

An additional possibility for the future of liquid interfacial nanoarchitectonics would be industrial applications. Many of the functions created by liquid interfacial nanoarchitectonics have potential applications ranging from biofunctions to device functions. Therefore, industrial applications should be considered as a goal. For this purpose, it is important to be able to mass produce at low cost. As seen in several examples, the use of emulsion

technology with a wide range of liquid–liquid interfaces is key. Nanoarchitectonics at the interface of emulsions dispersed at the micro- or nanoscale, rather than at the visible interface created by two immiscible solvents in a sample bottle, will pave the way for simple mass production. Methodologies such as emulsion nanoarchitectonics, which is an extension of liquid interfacial nanoarchitectonics, should be further developed. If such technologies can be developed, we can expect to see the creation of technologies that contribute to industrial applications while taking advantage of the two major characteristics of liquids and interfaces, as seen in the organization of biological systems.

Finally, several concluding remarks on more general points for further developments of nanoarchitectonics approach are described. Two issues necessitate consideration. The first necessity is the establishment of nanoarchitectonics processes based upon strong theoretical backgrounds. For example, the formation of assembled structures with amphiphiles can be interpreted by theoretical descriptions [393]. In addition, evaluation and analyses of assembling motifs can be supported by theory [394–396]. These theoretical methodologies must be aggressively used in nanoarchitectonics approaches. Another necessity is the integration of nanoarchitectonics into current science and technology. The use of nanoarchitectonics as a new concept in currently existing molecular and materials systems would be an efficient way to accelerate nanoarchitectonics approaches. For example, the integration of molecular construction with metallacycle [397–399] into nanoarchitectonics would result in fruitful outputs. The coupling of the new nanoarchitectonics concept and current science and technology would be an effective strategy for many current problems facing the energy, environmental, and biomedical fields. These practically effective approaches could become emerging trends in science and technology.

Funding: This study was partially supported by JSPS KAKENHI, grant number JP20H00392 and JP23H05459.

Acknowledgments: The author thanks Jerry Shen for his careful English correction and editing.

Conflicts of Interest: The author declares no conflicts of interest.

References

1. Kudo, A.; Miseki, Y. Heterogeneous photocatalyst materials for water splitting. *Chem. Soc. Rev.* **2009**, *38*, 253–278. [CrossRef] [PubMed]
2. Lang, X.; Hirata, A.; Fujita, T.; Chen, M. Nanoporous metal/oxide hybrid electrodes for electrochemical supercapacitors. *Nat. Nanotechnol.* **2011**, *6*, 232–236. [CrossRef] [PubMed]
3. Guo, D.; Shibuya, R.; Akiba, C.; Saji, S.; Kondo, T.; Nakamura, J. Active sites of nitrogen-doped carbon materials for oxygen reduction reaction clarified using model catalysts. *Science* **2016**, *351*, 361–365. [CrossRef] [PubMed]
4. Zhang, E.; Zhu, Q.; Huang, J.; Liu, J.; Tan, G.; Sun, C.; Li, T.; Liu, S.; Li, Y.; Wang, H.; et al. Visually resolving the direct Z-scheme heterojunction in CdS@$ZnIn_2S_4$ hollow cubes for photocatalytic evolution of H_2 and H_2O_2 from pure water. *Appl. Catal. B Environ.* **2021**, *293*, 120213. [CrossRef]
5. Saidul Islam, M.S.; Shudo, Y.; Hayami, S. Energy conversion and storage in fuel cells and super-capacitors from chemical modifications of carbon allotropes: State-of-art and prospect. *Bull. Chem. Soc. Jpn.* **2022**, *95*, 1–25. [CrossRef]
6. Yoshino, A. The lithium-ion battery: Two breakthroughs in development and two reasons for the Nobel prize. *Bull. Chem. Soc. Jpn.* **2022**, *95*, 195–197. [CrossRef]
7. Hosaka, T.; Komaba, S. Development of nonaqueous electrolytes for high-voltage K-ion batteries. *Bull. Chem. Soc. Jpn.* **2022**, *95*, 569–581. [CrossRef]
8. Xiao, J.; Hisatomi, T.; Kazunari Domen, K. Narrow-band-gap particulate photocatalysts for one-step-excitation overall water splitting. *Acc. Chem. Res.* **2023**, *56*, 878–888. [CrossRef] [PubMed]
9. Takeuchi, Y.; Matsuzawa, K.; Nagai, T.; Ikegami, K.; Kuroda, Y.; Monden, R.; Ishihara, A. Fe, N-Doped $SrTiO_3$ synthesized using pyrazine carboxylic acid-metal complexes: Application as an oxygen reduction catalyst for polymer electrolyte fuel cell cathodes in acidic media. *Bull. Chem. Soc. Jpn.* **2023**, *96*, 175–177. [CrossRef]
10. Fu, M.; Chen, W.; Lei, Y.; Yu, H.; Lin, Y.; Terrones, M. Biomimetic construction of ferrite quantum dot/graphene heterostructure for enhancing ion/charge transfer in supercapacitors. *Adv. Mater.* **2023**, *35*, 2300940. [CrossRef]
11. Ishihara, S.; Labuta, J.; Nakanishi, T.; Tanaka, T.; Kataura, H. Amperometric detection of sub-ppm formaldehyde using single-walled carbon nanotubes and hydroxylamines: A referenced chemiresistive system. *ACS Sens.* **2017**, *2*, 1405–1409. [CrossRef] [PubMed]

12. Zhuge, Z.; Liu, X.; Chen, T.; Gong, Y.; Li, C.; Niu, L.; Xu, S.; Xu, X.; Alothman, Z.A.; Sun, C.Q.; et al. Highly efficient photocatalytic degradation of different hazardous contaminants by $CaIn_2S_4$-$Ti_3C_2T_x$ Schottky heterojunction: An experimental and mechanism study. *Chem. Eng. J.* **2021**, *421*, 127838. [CrossRef]
13. Chapman, A.; Ertekin, E.; Kubota, M.; Nagao, A.; Bertsch, K.; Macadre, A.; Tsuchiyama, T.; Masamura, T.; Takaki, S.; Komoda, R.; et al. Achieving a carbon neutral future through advanced functional materials and technologies. *Bull. Chem. Soc. Jpn.* **2022**, *95*, 73–103. [CrossRef]
14. Shenashen, M.A.; Emran, M.Y.; Sabagh, A.E.; Selim, M.M.; Elmarakbi, A.; El-Safty, S.A. Progressin sensory devices of pesticides, pathogens, coronavirus, and chemical additives and hazards in food assessment: Food safety concerns. *Prog. Mater. Sci.* **2022**, *124*, 100866. [CrossRef]
15. Sasai, R.; Fujimura, T.; Sato, H.; Nii, E.; Sugata, M.; Nakayashiki, Y.; Hoashi, H.; Moriyosh, C.; Oishi, E.; Fujii, Y.; et al. Origin of selective nitrate removal by Ni^{2+}–Al^{3+} layered double hydroxides in aqueous media and its application potential in seawater purification. *Bull. Chem. Soc. Jpn.* **2022**, *95*, 802–812. [CrossRef]
16. Zhu, S.; Khan, M.A.; Kameda, T.; Xu, H.; Wang, F.; Xia, M.; Yoshioka, T. New insights into the capture performance and mechanism of hazardous metals Cr^{3+} and Cd^{2+} onto an effective layered double hydroxide based material. *J. Hazard. Mater.* **2022**, *426*, 128062. [CrossRef] [PubMed]
17. Ren, F.; He, R.; Ren, J.; Tao, F.; Yang, H.; Lv, H.; Ju, X. A friendly UV-responsive fluorine-free superhydrophobic coating for oil-water separation and dye degradation. *Bull. Chem. Soc. Jpn.* **2022**, *95*, 1091–1099. [CrossRef]
18. Mamun, M.R.A.; Yusuf, M.A.; Bhuyan, M.M.; Bhuiyan, M.S.H.; Arafath, M.A.; Uddin, M.N.; Soeb, M.J.A.; Almahri, A.; Rahman, M.M.; Karim, M.R. Acidity controlled desulfurization of biogas by using iron (III) and ferrosoferric (II, III) oxide. *Bull. Chem. Soc. Jpn.* **2022**, *95*, 1234–1241. [CrossRef]
19. Suzuki, H.; Takahashi, K. Water purification by 2-dimensional dodecagonal nitride and graphenylene via first principles calculations. *ChemPhysChem* **2023**, *24*, e202300115. [CrossRef]
20. Zhang, l.; Chong, H.L.H.; Moh, P.Y.; Albaqami, M.D.; Tighezza, A.M.; Qin, C.; Ni, X.; Cao, J.; Xu, X.; Yamauchi, Y. β-FeOOH nanospindles as chloride-capturing electrodes for electrochemical faradic deionization of saline water. *Bull. Chem. Soc. Jpn.* **2023**, *96*, 306–309. [CrossRef]
21. Tiburcius, S.; Krishnan, K.; Patel, V.; Netherton, J.; Sathish, C.I.; Weidenhofer, J.; Yang, J.-H.; Verrills, N.M.; Karakoti, A.; Vinu, A. Triple surfactant assisted synthesis of novel core-shell mesoporous silica nanoparticles with high surface area for drug delivery for prostate cancer. *Bull. Chem. Soc. Jpn.* **2022**, *95*, 331–340. [CrossRef]
22. Maeki, M.; Uno, S.; Niwa, A.; Okada, Y.; Tokeshi, M. Microfluidic technologies and devices for lipid nanoparticle-based RNA delivery. *J. Control. Release* **2022**, *344*, 80–96. [CrossRef] [PubMed]
23. Pradipta, A.R.; Michiba, H.; Kubo, A.; Fujii, M.; Tanei, T.; Morimoto, K.; Shimazu, K.; Tanaka, K. The second-generation click-to-sense probe for intraoperative diagnosis of breast cancer tissues based on acrolein targeting. *Bull. Chem. Soc. Jpn.* **2022**, *95*, 421–426. [CrossRef]
24. Su, C.-H.; Soendoro, A.; Okayama, S.; Rahmania, F.J.; Nagai, T.; Imae, T.; Tsutsumiuchi, K.; Kawai, N. Drug release stimulated by magnetic field and light on magnetite- and carbon dot-loaded carbon nanohorn. *Bull. Chem. Soc. Jpn.* **2022**, *95*, 582–594. [CrossRef]
25. Canh, V.D.; Liu, M.; Sangsanont, J.; Katayama, H. Capsid integrity detection of pathogenic viruses in waters: Recent progress and potential future applications. *Sci. Total Environ.* **2022**, *827*, 154258. [CrossRef] [PubMed]
26. Komiyama, M. Molecular mechanisms of the medicines for COVID-19. *Bull. Chem. Soc. Jpn.* **2022**, *95*, 1308–1317. [CrossRef]
27. Hata, M.; Kadoya, Y.; Hitomi, Y.; Kodera, M. Burst of DNA double-strand breaks by dicopper(II) complex with a p-cresol-2,6-bis(amide-tether-dpa) ligand via reductive O_2-activation. *Bull. Chem. Soc. Jpn.* **2022**, *95*, 1546–1552. [CrossRef]
28. Yang, W.; Mixich, L.; Boonstra, E.; Cabral, H. Polymer-based mRNA delivery strategies for advanced therapies. *Adv. Healthc. Mater.* **2023**, *12*, 2202688. [CrossRef] [PubMed]
29. Suzuki, H.; Imajo, Y.; Funaba, M.; Ikeda, H.; Nishida, N.; Sakai, T. Current concepts of biomaterial scaffolds and regenerative therapy for spinal cord injury. *Int. J. Mol. Sci.* **2023**, *24*, 2528. [CrossRef]
30. Niwa, T.; Tahara, T.; Chase, C.E.; Fang, F.G.; Nakaoka, T.; Irie, S.; Hayashinaka, E.; Wada, Y.; Mukai, H.; Masutomi, K.; et al. Synthesis of ^{11}C-radiolabeled eribulin as a companion diagnostics PET tracer for brain glioblastoma. *Bull. Chem. Soc. Jpn.* **2023**, *96*, 283–290. [CrossRef]
31. Kumagai, S.; Koguma, T.; Annaka, T.; Sawabe, C.; Tani, Y.; Sugiura, H.; Watanabe, T.; Hashizume, D.; Takeya, J.; Okamoto, T. Regioselective functionalization of nitrogen-embedded perylene diimides for high-performance organic Electron-transporting materials. *Bull. Chem. Soc. Jpn.* **2022**, *95*, 953–960. [CrossRef]
32. Wang, S.; Yuan, J.; Wang, L.; Xiao, L.; Jia, S. All-optical information conversion in Rb vapor based on the spatial cross-phase modulation. *Opt. Express* **2022**, *30*, 45517–45524. [CrossRef] [PubMed]
33. Saito, Y.; Sasabe, H.; Tsuneyama, H.; Abe, S.; Matsuya, M.; Kawano, T.; Kori, Y.; Hanayama, T.; Kido, J. Quinoline-modified phenanthroline electron-transporters as n-type exciplex partners for highly efficient and stable deep-red OLEDs. *Bull. Chem. Soc. Jpn.* **2023**, *96*, 24–28. [CrossRef]
34. Liang, F.-C.; Jhuang, F.-C.; Fang, Y.-H.; Benas, J.-S.; Chen, W.-C.; Yan, Z.-L.; Lin, W.-C.; Su, C.-J.; Sato, Y.; Chiba, T.; et al. Synergistic effect of cation composition engineering of hybrid $Cs_{1-x}FA_xPbBr_3$ nanocrystals for self-healing electronics application. *Adv. Mater.* **2023**, *35*, 2207617. [CrossRef] [PubMed]

35. Matsuya, M.; Sasabe, H.; Sumikoshi, S.; Hoshi, K.; Nakao, K.; Kumada, K.; Sugiyama, R.; Sato, R.; Kido, J. Highly Luminescent aluminum complex with β-diketone ligands exhibiting near-unity photoluminescence quantum yield, thermally activated delayed fluorescence, and rapid radiative decay rate properties in solution-processed organic light-emitting devices. *Bull. Chem. Soc. Jpn.* **2023**, *96*, 183–189. [CrossRef]
36. Yu, C.P.; Kumagai, S.; Tsutsumi, M.; Kurosawa, T.; Ishii, H.; Watanabe, G.; Hashizume, D.; Sugiura, H.; Tani, Y.; Ise, T.; et al. Asymmetrically functionalized electron-deficient π-conjugated system for printed single-crystalline organic electronics. *Adv. Sci.* **2023**, *10*, 2207440. [CrossRef] [PubMed]
37. Kim, S.; Ju, D.; Kim, S. Implementation of artificial synapse using IGZO-based resistive switching device. *Materials* **2024**, *17*, 481. [CrossRef]
38. Kwon, C.; Kang, D. Overlay-ML: Unioning memory and storage space for on-device AI on mobile devices. *Appl. Sci.* **2024**, *14*, 3022. [CrossRef]
39. D'Avenio, G.; Daniele, C.; Grigioni, M. Nanostructured medical devices: Regulatory perspective and current applications. *Materials* **2024**, *17*, 1787. [CrossRef]
40. Park, J.; Shin, J.; Yoo, H. Heterostructure-based optoelectronic neuromorphic devices. *Electronics* **2024**, *13*, 1076. [CrossRef]
41. Simons, K.; Toomre, D. Lipid rafts and signal transduction. *Nat. Rev. Mol. Cell Biol.* **2000**, *1*, 31–39. [CrossRef] [PubMed]
42. Vetter, I.R.; Wittinghofer, A. Signal transduction-The guanine nucleotide-binding switch in three dimensions. *Science* **2001**, *294*, 1299–1304. [CrossRef] [PubMed]
43. Ferreira, K.N.; Iverson, T.M.; Maghlaoui, K.; Barber, J.; Iwata, S. Architecture of the photosynthetic oxygen-evolving center. *Science* **2004**, *303*, 1831–1838. [CrossRef] [PubMed]
44. Shen, J.-R. The structure of photosystem II and the mechanism of water oxidation in photosynthesis. *Ann. Rev. Plant Biol.* **2015**, *66*, 23–48. [CrossRef] [PubMed]
45. Povie, G.; Segawa, Y.; Nishihara, T.; Miyauchi, Y.; Itami, K. Synthesis of a carbon nanobelt. *Science* **2017**, *356*, 172–175. [CrossRef] [PubMed]
46. Sun, Z.; Ikemoto, K.; Fukunaga, T.M.; Koretsune, T.; Arita, R.; Sato, S.; Isobe, H. Finite phenine nanotubes with periodic vacancy defects. *Science* **2019**, *363*, 151–154. [CrossRef] [PubMed]
47. Sugiyama, M.; Akiyama, M.; Yonezawa, Y.; Komaguchi, K.; Higashi, M.; Nozaki, K.; Okazoe, T. Electron in a cube: Synthesis and characterization of perfluorocubane as an electron acceptor. *Science* **2022**, *377*, 756–759. [CrossRef] [PubMed]
48. Hirano, K. Copper-catalyzed electrophilic amination: An umpolung strategy for new C–N bond formations. *Bull. Chem. Soc. Jpn.* **2023**, *96*, 198–207. [CrossRef]
49. Tsubaki, N.; Wang, Y.; Yang, G.; He, Y. Rational design of novel reaction pathways and tailor-made catalysts for value-added chemicals synthesis from CO_2 hydrogenation. *Bull. Chem. Soc. Jpn.* **2023**, *96*, 291–302. [CrossRef]
50. Kobayashi, T.; Sakurai, T.; Kumagai, N. Peripheral modification of tripodal aza-oxa-crown oxa-triquinoline. *Bull. Chem. Soc. Jpn.* **2023**, *96*, 1139–1143. [CrossRef]
51. Wang, W.; Yu, L. Synthesis of indenones via persulfate promoted radical alkylation/cyclization of biaryl ynones with 1,4-dihydropyridines. *Molecules* **2024**, *29*, 458. [CrossRef] [PubMed]
52. Scarpelli, R.; Bence, R.; Cano, N.C.H.; Procopio, A.; Wunderlin, D.; Nardi, M. A Review on the use of deep eutectic solvents in protection reactions. *Molecules* **2024**, *29*, 818. [CrossRef] [PubMed]
53. Xu, J. Recent advances in π-stacking interaction-controlled asymmetric synthesis. *Molecules* **2024**, *29*, 1454. [CrossRef] [PubMed]
54. Yamaoka, Y.; Miyabe, H. NHC-catalyzed reaction of aldehydes for C(sp^2)–O bond formation. *Catalysts* **2024**, *14*, 219. [CrossRef]
55. Tanaka, T. Synthesis of novel heteronanographenes via fold-in approach. *Bull. Chem. Soc. Jpn.* **2022**, *95*, 602–610. [CrossRef]
56. Yoshino, S.; Iwase, A.; Yamaguchi, Y.; Suzuki, T.M.; Morikawa, T.; Kudo, A. Photocatalytic CO_2 reduction using water as an electron donor under visible light irradiation by Z-scheme and photoelectrochemical systems over $(CuGa)_{0.5}ZnS_2$ in the presence of basic additives. *J. Am. Chem. Soc.* **2022**, *144*, 2323–2332. [CrossRef] [PubMed]
57. Negishi, Y. Metal-nanocluster science and technology: My personal history and outlook. *Phys. Chem. Chem. Phys.* **2022**, *24*, 7569–7594. [CrossRef] [PubMed]
58. Tanks, J.; Hiroi, T.; Tamura, K.; Naito, K. Tethering organic disulfides to layered silicates: A versatile strategy for photo-controllable dynamic chemistry and functionalization. *Bull. Chem. Soc. Jpn.* **2023**, *96*, 65–71. [CrossRef]
59. Okamoto, K.; Imoto, H.; Naka, K. Silsesquioxane cage-fused siloxane rings as a novel class of inorganic-based host molecules. *Bull. Chem. Soc. Jpn.* **2023**, *96*, 84–89. [CrossRef]
60. Takeuchi, Y.; Ohkura, K.; Nishina, Y. Self-assembly strategies for graphene oxide/silica nanostructures: Synthesis and structural analysis. *Bull. Chem. Soc. Jpn.* **2023**, *96*, 113–119. [CrossRef]
61. Minamihara, H.; Kusada, K.; Yamamoto, T.; Toriyama, T.; Murakami, Y.; Matsumura, S.; Kumara, L.S.R.; Sakata, O.; Kawaguchi, S.; Kubota, Y.; et al. Continuous-flow chemical synthesis for sub-2 nm ultra-multielement alloy nanoparticles consisting of group IV to XV elements. *J. Am. Chem. Soc.* **2023**, *145*, 17136–17142. [CrossRef] [PubMed]
62. Zhang, G.; Bai, Q.; Wang, X.; Li, C.; Uyama, H.; Shen, Y. Preparation and mechanism investigation of walnut shell-based hierarchical porous carbon for supercapacitors. *Bull. Chem. Soc. Jpn.* **2023**, *96*, 190–197. [CrossRef]
63. Teplonogova, M.A.; Kozlova, A.A.; Yapryntsev, A.D.; Baranchikov, A.E.; Ivanov, V.K. Synthesis and thermal decomposition of high-entropy layered rare earth hydroxychlorides. *Molecules* **2024**, *29*, 1634. [CrossRef] [PubMed]

64. Yin, C.; Li, Y.; Yu, J.; Deng, Z.; Liu, S.; Shi, X.; Tang, D.; Chen, X.; Zhang, L. Dragon's blood-loaded mesoporous silica nanoparticles for rapid hemostasis and antibacterial activity. *Molecules* **2024**, *29*, 1888. [CrossRef] [PubMed]
65. Liu, C.; Morimoto, N.; Jiang, L.; Kawahara, S.; Noritomi, T.; Yokoyama, H.; Mayumi, K.; Ito, K. Tough hydrogels with rapid self-reinforcement. *Science* **2021**, *372*, 1078–1081. [CrossRef] [PubMed]
66. Zhang, D.; Liu, D.; Ubukata, T.; Seki, T. Unconventional approaches to light-promoted dynamic surface morphing on polymer films. *Bull. Chem. Soc. Jpn.* **2022**, *95*, 138–162. [CrossRef]
67. Nishijima, A.; Kametani, Y.; Uemura, T. Reciprocal regulation between MOFs and polymers. *Coord. Chem. Rev.* **2022**, *466*, 214601. [CrossRef]
68. Mori, H.; Yamada, Y.; Minagawa, Y.; Hasegawa, N.; Nishihara, Y. Effects of acyloxy groups in anthrabisthiadiazole-based semiconducting polymers on electronic properties, thin-film structure, and solar cell performance. *Bull. Chem. Soc. Jpn.* **2022**, *95*, 942–952. [CrossRef]
69. Kato, K.; Seto, N.; Chida, K.; Yoshii, T.; Mizuno, M.; Nishihara, H.; Ohtani, S.; Ogoshi, T. Synthesis of hexa-aminated trinaphtho[3.3.3]propellane and its porous polymer solids with alkane adsorption properties. *Bull. Chem. Soc. Jpn.* **2022**, *95*, 1296–1302. [CrossRef]
70. Watanabe, H.; Kamigaito, M. Direct radical copolymerizations of thioamides to generate vinyl polymers with degradable thioether bonds in the backbones. *J. Am. Chem. Soc.* **2023**, *145*, 10948–10953. [CrossRef]
71. Hosokawa, S.; Nagao, A.; Hashimoto, Y.; Matsune, A.; Okazoe, T.; Suzuki, C.; Wada, H.; Kakiuchi, T.; Tsuda, A. Non-Isocyanate polyurethane synthesis by polycondensation of alkylene and arylene bis(fluoroalkyl) bis(carbonate)s with diamines. *Bull. Chem. Soc. Jpn.* **2023**, *96*, 663–670. [CrossRef]
72. Bouzayani, B.; Sanromán, M.Á. Polymer-supported heterogeneous Fenton catalysts for the environmental remediation of wastewater. *Molecules* **2024**, *29*, 2188. [CrossRef] [PubMed]
73. Abdelmoteleb, K.M.A.; Wasfy, A.A.F.; El-Apasery, M.A. Novel disperse dyes based on enaminones: Synthesis, dyeing performance on polyester fabrics, and potential biological activities. *Molecules* **2024**, *29*, 2227. [CrossRef]
74. Aldosari, S.M.; AlOtaibi, B.M.; Alblalaihid, K.S.; Aldoihi, S.A.; AlOgab, K.A.; Alsaleh, S.S.; Alshamary, D.O.; Alanazi, T.H.; Aldrees, S.D.; Alshammari, B.A. Mechanical recycling of carbon fiber-reinforced polymer in a circular economy. *Polymers* **2024**, *16*, 1363. [CrossRef] [PubMed]
75. Datta, S.; Kato, Y.; Higashiharaguchi, S.; Aratsu, K.; Isobe, A.; Saito, T.; Prabhu, D.D.; Kitamoto, Y.; Hollamby, M.J.; Smith, A.J.; et al. Self-assembled poly-catenanes from supramolecular toroidal building blocks. *Nature* **2020**, *583*, 400–405. [CrossRef]
76. Baba, K.; Nagata, K.; Yajima, T.; Yoshimura, T. Synthesis, structures, and equilibrium reactions of La(III) and Ba(II) complexes with pyridine phosphonate pendant arms on a diaza-18-crown-6 ether. *Bull. Chem. Soc. Jpn.* **2022**, *95*, 466–475. [CrossRef]
77. Oki, O.; Yamagishi, H.; Morisaki, Y.; Inoue, R.; Ogawa, K.; Miki, N.; Norikane, Y.; Sato, H.; Yamamoto, Y. Synchronous assembly of chiral skeletal single-crystalline microvessels. *Science* **2022**, *377*, 673–677. [CrossRef]
78. Han, X.; Wang, S.; Liu, M.; Liu, L. A cucurbit[6]uril-based supramolecular assembly as a multifunctional material for the detection and removal of organic explosives and antibiotics. *Bull. Chem. Soc. Jpn.* **2022**, *95*, 1445–1452. [CrossRef]
79. Mukhopadhyay, R.D.; Ajayaghosh, A. Metallosupramolecular polymers: Current status and future prospects. *Chem. Soc. Rev.* **2023**, *52*, 8635–8650. [CrossRef]
80. Kubota, R. Supramolecular–polymer composite hydrogels: From In Situ network observation to functional properties. *Bull. Chem. Soc. Jpn.* **2023**, *96*, 802–812. [CrossRef]
81. Jansen, S.A.H.; Weyandt, E.; Aoki, T.; Akiyama, T.; Itoh, Y.; Vantomme, G.; Aida, T.; Meijer, E.W. Simulating assembly landscapes for comprehensive understanding of supramolecular polymer–solvent systems. *J. Am. Chem. Soc.* **2023**, *145*, 4231–4237. [CrossRef] [PubMed]
82. He, Q.; Wei, L.; He, C.; Yang, C.; Wu, W. Supramolecular annihilator with DPA parallelly arranged by multiple hydrogen-bonding interactions for enhanced triplet–triplet annihilation upconversion. *Molecules* **2024**, *29*, 2203. [CrossRef] [PubMed]
83. Hu, M.; Bao, J.; Zhang, Y.; Wang, L.; Zhang, Y.; Zhang, J.; Tang, J.; Zou, Q. Supramolecular nanoparticles of histone and hyaluronic acid for co-delivery of siRNA and photosensitizer in vitro. *Int. J. Mol. Sci.* **2024**, *25*, 5424. [CrossRef] [PubMed]
84. Kuppadakkath, G.; Jayabhavan, S.S.; Damodaran, K.K. Supramolecular Gels Based on C_3-symmetric amides: Application in anion-sensing and removal of dyes from water. *Molecules* **2024**, *29*, 2149. [CrossRef] [PubMed]
85. Bennett, T.D.; Horike, S. Liquid, glass and amorphous solid states of coordination polymers and metal–organic frameworks. *Nat. Rev. Mater.* **2018**, *3*, 431–440. [CrossRef]
86. Gu, Y.; Zheng, J.-J.; Otake, K.; Shivanna, M.; Sakaki, S.; Yoshino, H.; Ohba, M.; Kawaguchi, S.; Wang, Y.; Li, F.; et al. Host–guest interaction modulation in porous coordination polymers for inverse selective CO_2/C_2H_2 separation. *Angew. Chem. Int. Ed.* **2021**, *60*, 11688. [CrossRef] [PubMed]
87. Shan, Y.; Zhang, G.; Yin, W.; Pang, H.; Xu, Q. Recent progress in Prussian blue/Prussian blue analogue-derived metallic compounds. *Bull. Chem. Soc. Jpn.* **2022**, *95*, 230–260. [CrossRef]
88. Domoto, Y.; Fujita, M. Self-assembly of nanostructures with high complexity based on metal· · · unsaturated-bond coordination, Coordination. *Chem. Rev.* **2022**, *466*, 214605. [CrossRef]
89. Yam, V.W.-W.; Cheng, Y.-H. Stimuli-responsive and switchable platinum(II) complexes and their applications in memory storage. *Bull. Chem. Soc. Jpn.* **2022**, *95*, 846–854. [CrossRef]

90. Shivanna, M.; Otake, K.; Hiraide, S.; Fujikawa, T.; Wang, P.; Gu, Y.; Ashitani, H.; Kawaguchi, S.; Kubota, Y.; Miyahara, M.T.; et al. Crossover sorption of C_2H_2/CO_2 and C_2H_6/C_2H_4 in soft porous coordination networks. *Angew. Chem. Int. Ed.* **2023**, *62*, e202308438. [CrossRef]
91. Miles-Hobbs, A.M.; Pringle, P.G.; Woollins, J.D.; Good, D. Monofluorophos–metal gomplexes: Ripe for future discoveries in homogeneous catalysis. *Molecules* **2024**, *29*, 2368. [CrossRef] [PubMed]
92. Plasseraud, L. Glycerol as ligand in metal complexes—A structural review. *Crystals* **2024**, *14*, 217. [CrossRef]
93. Chiacchio, M.A.; Campisi, A.; Iannazzo, D.; Giofrè, S.V.; Legnani, L. Design of new Schiff bases and their heavy metal ion complexes for environmental applications: A molecular dynamics and density function theory study. *Int. J. Mol. Sci.* **2024**, *25*, 4159. [CrossRef] [PubMed]
94. Aitken, R.A.; Dawson, G.; Keddie, N.S.; Kraus, H.; Milton, H.L.; Slawin, A.M.Z.; Wheatley, J.; Woollins, J.D. Thermal rearrangement of thiocarbonyl-stabilised triphenylphosphonium ylides leading to (Z)-1-diphenylphosphino-2-(phenylsulfenyl)alkenes and their coordination chemistry. *Molecules* **2024**, *29*, 221. [CrossRef] [PubMed]
95. Hanamura, M.; Sawada, T.; Serizawa, T. In-paper self-assembly of cellulose oligomers for the preparation of all-cellulose functional paper. *ACS Sustain. Chem. Eng.* **2021**, *9*, 5684–5692. [CrossRef]
96. Tamura, T.; Inoue, M.; Yoshimitsu, Y.; Hashimoto, I.; Ohashi, N.; Tsumura, K.; Suzuki, K.; Watanabe, T.; Hohsaka, T. Chemical synthesis and cell-free expression of thiazoline ring-bridged cyclic Peptides and their properties on biomembrane permeability. *Bull. Chem. Soc. Jpn.* **2022**, *95*, 359–366. [CrossRef]
97. Sato, R.; Amao, Y. Curious effect of isotope-labelled substrate/Co-enzyme on catalytic Activity of CO_2 reduction by formate dehydrogenase from *Candida boidinii*. *Bull. Chem. Soc. Jpn.* **2022**, *95*, 556–558. [CrossRef]
98. Inaba, H.; Sueki, Y.; Ichikawa, M.; Kabir, A.M.R.; Iwasaki, T.; Shigematsu, H.; Kakugo, A.; Sada, K.; Tsukazaki, T.; Matsuura, K. Generation of stable microtubule superstructures by binding of peptide-fused tetrameric proteins to inside and outside. *Sci. Adv.* **2022**, *8*, eabq3817. [CrossRef]
99. Sahayasheela, V.J.; Yu, Z.; Hirose, Y.; Pandian, G.N.; Bando, T.; Sugiyama, H. Inhibition of GLI-mediated transcription by cyclic pyrrole-imidazole polyamide in cancer stem cells. *Bull. Chem. Soc. Jpn.* **2022**, *95*, 693–699. [CrossRef]
100. Negi, S.; Hamori, M.; Sato, A.; Shimizu, K.; Kawahara-Nakagawa, Y.; Manabe, T.; Shibata, N.; Kitagishi, H.; Mashimo, M.; Sugiura, Y. Transpeptidation reaction mediated by ligand- and metal cofactor-substituted sortase A from *Staphylococcus aureus*. *Bull. Chem. Soc. Jpn.* **2022**, *95*, 1025–1031. [CrossRef]
101. Inaba, H.; Hori, Y.; Kabir, A.M.R.; Kakugo, A.; Sada, K.; Matsuura, K. Construction of silver nanoparticles inside microtubules using Tau-derived peptide ligated with silver-binding peptide. *Bull. Chem. Soc. Jpn.* **2023**, *96*, 1082–1087. [CrossRef]
102. Rossi-Gendron, C.; Fakih, F.E.; Bourdon, L.; Nakazawa, K.; Finkel, J.; Triomphe, N.; Chocron, L.; Endo, M.; Sugiyama, H.; Bellot, C.; et al. Isothermal self-assembly of multicomponent and evolutive DNA nanostructures. *Nat. Nanotechnol.* **2023**, *18*, 1311–1318. [CrossRef] [PubMed]
103. Mohanan, S.; Sathish, C.I.; Adams, T.J.; Kan, S.; Liang, M.; Vinu, A. A dual protective drug delivery system based on lipid coated core-shell mesoporous silica for efficient delivery of cabazitaxel to prostate cancer cells. *Bull. Chem. Soc. Jpn.* **2023**, *96*, 1188–1195. [CrossRef]
104. Scheim, D.E.; Parry, P.I.; Rabbolini, D.J.; Aldous, C.; Yagisawa, M.; Clancy, R.; Borody, T.J.; Hoy, W.E. Back to the basics of SARS-CoV-2 biochemistry: Microvascular occlusive glycan bindings govern its morbidities and inform therapeutic responses. *Viruses* **2024**, *16*, 647. [CrossRef]
105. Maeda, K.; Takeiri, F.; Kobayashi, G.; Matsuishi, S.; Ogino, H.; Ida, S.; Mori, T.; Uchimoto, Y.; Tanabe, S.; Hasegawa, T.; et al. Recent progress on mixed-anion materials for energy applications. *Bull. Chem. Soc. Jpn.* **2022**, *95*, 26–37. [CrossRef]
106. Gilbert, P.U.P.A.; Bergmann, K.D.; Boekelheide, N.; Tambutté, S.; Mass, T.; Marin, F.; Adkins, J.F.; Erez, J.; Gilbert, B.; Knutson, V.; et al. Biomineralization: Integrating mechanism and evolutionary history. *Sci. Adv.* **2022**, *8*, eabl9653. [CrossRef] [PubMed]
107. Kurniawan, E.; Hara, T.; Permana, Y.; Kojima, T.; Ichikuni, N.; Shimazu, S. Creation of highly reducible CuO species by high-temperature calcination of a Cu-Al layered double hydroxide: Selective hydrogenation of furfural into furfuryl alcohol with formic acid. *Bull. Chem. Soc. Jpn.* **2022**, *95*, 121–128. [CrossRef]
108. Antonova, I.V.; Seleznev, V.A.; Nebogatikova, N.A.; Ivanov, A.I.; Voloshin, B.V.; Volodin, V.A.; Kurkina, I.I. Thin V_2O_5 films synthesized by plasma-enhanced atomic layer deposition for memristive applications. *Phys. Chem. Chem. Phys.* **2023**, *25*, 32132–32141. [CrossRef]
109. Adschiri, T.; Takami, S.; Umetsu, M.; Ohara, S.; Naka, T.; Minami, K.; Hojo, D.; Togashi, T.; Arita, T.; Taguchi, M.; et al. Supercritical hydrothermal reactions for material synthesis. *Bull. Chem. Soc. Jpn.* **2023**, *96*, 133–147. [CrossRef]
110. Wang, D.; Jiang, W.; Li, S.; Yan, X.; Wu, S.; Qiu, H.; Guo, S.; Zhu, B. A comprehensive review on combinatorial film via high-throughput techniques. *Materials* **2023**, *16*, 6696. [CrossRef] [PubMed]
111. Saito, K.; Yamamura, Y. Reticular-chemical approach to soft-matter self-assembly: Why are srs and noh nets realized in thermotropics? *Bull. Chem. Soc. Jpn.* **2023**, *96*, 607–613. [CrossRef]
112. Murayama, K.; Okita, H.; Asanuma, H. Highly functional acyclic xeno nucleic acids. *Bull. Chem. Soc. Jpn.* **2023**, *96*, 1179–1187. [CrossRef]
113. Ariga, K.; Akakabe, S.; Sekiguchi, R.; Thomas, M.I.; Takeoka, Y.; Rikukawa, M.; Yoshizawa-Fujita, M. Boosting the ionic conductivity of pyrrolidinium-based ionic plastic crystals by LLZO fillers. *ACS Omega* **2024**, *9*, 22203–22212. [CrossRef] [PubMed]

114. Shpotyuk, O.; Lukáčová Bujňáková, Z.; Baláž, P.; Kovalskiy, A.; Sznajder, M.; Cebulski, J.; Shpotyuk, Y.; Demchenko, P.; Syvorotka, I. Equimolar As_4S_4/Fe_3O_4 nanocomposites fabricated by dry and wet mechanochemistry: Some insights on the magnetic–fluorescent functionalization of an old drug. *Materials* **2024**, *17*, 1726. [CrossRef] [PubMed]
115. Imai, Y.; Mimura, Y.; Motomura, Y.; Ikemura, R.; Shizuma, M.; Kitamatsu, M. Controlling excimer-origin circularly polarized luminescence of bipyrenyl-arginine peptides by cyclodextrin in water. *Bull. Chem. Soc. Jpn.* **2023**, *96*, 268–273. [CrossRef]
116. Mieda, E.; Morishima, Y.; Watanabe, T.; Miyake, H.; Shinoda, S. Synthesis and luminescence properties of self-assembled lanthanide complexes with an EDTA-type chelating ligand in aqueous ethanol solution. *Bull. Chem. Soc. Jpn.* **2023**, *96*, 538–544. [CrossRef]
117. Nguyen, L.T.B.; Abe, M. Development of photoremovable protecting groups responsive to near-infrared two-photon excitation and their application to drug delivery research. *Bull. Chem. Soc. Jpn.* **2023**, *96*, 899–906. [CrossRef]
118. Li, Y.; Zhao, C.; Wang, Z.; Zeng, Y. Halogen bond catalysis: A physical chemistry perspective. *J. Phys. Chem. A* **2024**, *128*, 507–527. [CrossRef]
119. Salahuddin, B.; Masud, M.K.; Aziz, S.; Liu, C.-H.; Amiralian, N.; Ashok, A.; Hossain, S.M.A.; Park, H.; Wahab, M.A.; Amin, M.A.; et al. κ-Carrageenan gel modified mesoporous gold chronocoulometric sensor for ultrasensitive detection of microRNA. *Bull. Chem. Soc. Jpn.* **2022**, *95*, 198–207. [CrossRef]
120. Murata, T.; Minami, K.; Yamazaki, T.; Sato, T.; Koinuma, H.; Ariga, K.; Matsuki, N. Nanometer-flat DNA-featured thin films prepared via laser molecular beam deposition under high-vacuum for selective methanol sensing. *Bull. Chem. Soc. Jpn.* **2023**, *96*, 29–34. [CrossRef]
121. Kalyana Sundaram, S.d.; Hossain, M.M.; Rezki, M.; Ariga, K.; Tsujimura, S. Enzyme cascade electrode reactions with nanomaterials and their applicability towards biosensor and biofuel cells. *Biosensors* **2023**, *13*, 1018. [CrossRef] [PubMed]
122. Cheng, B.; Hu, K.; Song, Z.; An, R.; Liang, X. Nanopore sequencing of short dsDNA after elongation by combination of ligation and PEAR. *Bull. Chem. Soc. Jpn.* **2023**, *96*, 785–792. [CrossRef]
123. Yao, D.; Xia, L.; Li, G. Research progress on the application of covalent organic framework nanozymes in analytical chemistry. *Biosensors* **2024**, *14*, 163. [CrossRef] [PubMed]
124. Lin, H.; Yu, J.; Chen, F.; Li, R.; Xia, B.Y.; Xu, Z.-L. Visualizing the interfacial chemistry in multivalent metal anodes by transmission electron microscopy. *Small Methods* **2023**, *7*, 2300561. [CrossRef] [PubMed]
125. Miadonye, A.; Amadu, M. Theoretical interpretation of pH and salinity effect on oil-in-water emulsion stability based on interfacial chemistry and implications for produced water demulsification. *Processes* **2023**, *11*, 2470. [CrossRef]
126. Kong, Y.; Ma, S.; Zhou, F. Bioinspired interfacial friction control: From chemistry to structures to mechanics. *Biomimetics* **2024**, *9*, 200. [CrossRef] [PubMed]
127. Huang, Y.; Geng, J.; Zhang, T.; Jiang, Z.; Fang, H.; Hua, W.; Li, F. Interfacial chemistry regulation using functional frameworks for stable metal batteries. *J. Mater. Chem. A* **2024**, *12*, 5080–5099. [CrossRef]
128. Lu, Y.; Ni, Y.; Chen, J. Reliable organic carbonyl electrode materials enabled by electrolyte and interfacial chemistry regulation. *Acc. Chem. Res.* **2024**, *57*, 375–385. [CrossRef] [PubMed]
129. Tokoro, H.; Nakabayashi, K.; Nagashima, S.; Song, Q.; Yoshikiyo, M.; Ohkoshi, S. Optical properties of epsilon iron oxide nanoparticles in the millimeter- and terahertz-wave regions. *Bull. Chem. Soc. Jpn.* **2022**, *95*, 538–552. [CrossRef]
130. Yamamoto, Y.; Nakano, S.; Shigeta, Y. Dynamical interaction analysis of proteins by a random forest-fragment molecular orbital (RF-FMO) method and application to Src tyrosine kinase. *Bull. Chem. Soc. Jpn.* **2023**, *96*, 42–47. [CrossRef]
131. Yasui, K.; Hamamoto, K. Possibility of high ionic conductivity and high fracture toughness in all-dislocation-ceramics. *Materials* **2024**, *17*, 428. [CrossRef] [PubMed]
132. Ii, S. Quantitative characterization by transmission electron microscopy and its application to interfacial phenomena in crystalline materials. *Materials* **2024**, *17*, 578. [CrossRef] [PubMed]
133. Hieda, M.; Tsujimura, K.; Kinoshita, M.; Matsumori, N. Formation of a tight complex between amphidinol and sterols in lipid bilayers revealed by short-range energy transfer. *Bull. Chem. Soc. Jpn.* **2022**, *95*, 1753–1759. [CrossRef]
134. Imahori, H. Molecular photoinduced charge separation: Fundamentals and application. *Bull. Chem. Soc. Jpn.* **2023**, *96*, 339–352. [CrossRef]
135. Kuzume, A.; Yamamoto, K. Dendrimer-induced synthesis of subnano materials and their characterization: Establishing atom hybrid science. *Bull. Chem. Soc. Jpn.* **2024**, *97*, uoae022. [CrossRef]
136. Sugimoto, Y.; Pou, P.; Abe, M.; Jelinek, P.; Pérez, R.; Morita, S.; Custance, Ó. Chemical identification of individual surface atoms by atomic force microscopy. *Nature* **2007**, *446*, 64–67. [CrossRef]
137. Kawai, S.; Krejcí, O.; Nishiuchi, T.; Sahara, K.; Kodama, T.; Pawlak, R.; Meyer, E.; Kubo, T.; Foster, A.S. Three-dimensional graphene nanoribbons as a framework for molecular assembly and local probe chemistry. *Sci. Adv.* **2020**, *6*, eaay8913. [CrossRef]
138. Seo, D.; Seong, S.; Kim, H.; Oh, H.S.; Lee, J.H.; Kim, H.; Kim, Y.O.; Maeda, S.; Chikami, S.; Hayashi, T.; et al. Molecular self-assembly and adsorption structure of 2,2′-dipyrimidyl dDisulfides on Au(111) surfaces. *Molecules* **2024**, *29*, 846. [CrossRef]
139. Fedorov, A.Y.; Bukhtiyarov, A.V.; Panafidin, M.A.; Prosvirin, I.P.; Zubavichus, Y.V.; Bukhtiyarov, V.I. Thermally Induced surface structure and morphology evolution in bimetallic Pt-Au/HOPG nanoparticles as probed using XPS and STM. *Nanomaterials* **2024**, *14*, 57. [CrossRef]
140. Terabe, K.; Hasegawa, T.; Nakayama, T.; Aono, M. Quantized conductance atomic switch. *Nature* **2005**, *433*, 47–50. [CrossRef]

141. Kimura, K.; Miwa, K.; Imada, H.; Imai-Imada, M.; Kawahara, S.; Takeya, J.; Kawai, M.; Galperin, M.; Kim, Y. Selective triplet exciton formation in a single molecule. *Nature* **2019**, *570*, 210–213. [CrossRef]
142. Hashikawa, Y.; Murata, Y. Water in fullerenes. *Bull. Chem. Soc. Jpn.* **2023**, *96*, 943–967. [CrossRef]
143. Matsuno, T.; Isobe, H. Trapped yet Free inside the Tube: Supramolecular Chemistry of Molecular Peapods. *Bull. Chem. Soc. Jpn.* **2023**, *96*, 406–419. [CrossRef]
144. Ariga, K. Nanoarchitectonics: What's coming next after nanotechnology? *Nanoscale Horiz.* **2021**, *6*, 364–378. [CrossRef]
145. Feynman, R.P. There's plenty of room at the bottom. *Calif. Inst. Technol. J. Eng. Sci.* **1960**, *4*, 23–36.
146. Roukes, M. Plenty of room, indeed. *Sci. Am.* **2001**, *285*, 48–57. [CrossRef]
147. Ariga, K.; Minami, K.; Ebara, M.; Nakanishi, J. What are the emerging concepts and challenges in NANO? Nanoarchitectonics, hand-operating nanotechnology and mechanobiology. *Polym. J.* **2016**, *48*, 371–389. [CrossRef]
148. Ariga, K.; Aono, M. Nanoarchitectonics. *Jpn. J. Appl. Phys.* **2016**, *55*, 1102A6. [CrossRef]
149. Ariga, K.; Ji, Q.; Nakanishi, W.; Hill, J.P.; Aono, M. Nanoarchitectonics: A new materials horizon for nanotechnology. *Mater. Horiz.* **2015**, *2*, 406–413. [CrossRef]
150. Eftekhari, K.; Parakhonskiy, B.V.; Grigoriev, D.; Skirtach, A.G. Advances in nanoarchitectonics: A review of "static" and "dynamic" particle assembly methods. *Materials* **2024**, *17*, 1051. [CrossRef]
151. Shimada, S.; Miyagishi, H.V.; Masai, H.; Masui, Y.; Terao, J. Solvatofluorochromic contrast with supramolecular stereoisomers using linked rotaxane structures to investigate local solvation in excited donor-bridge-acceptor systems. *Bull. Chem. Soc. Jpn.* **2022**, *95*, 163–168. [CrossRef]
152. Hamada, K.; Shimoyama, D.; Hirao, T.; Haino, T. Chiral supramolecular polymer formed via host-guest complexation of an octaphosphonate biscavitand and a chiral diammonium guest. *Bull. Chem. Soc. Jpn.* **2022**, *95*, 621–627. [CrossRef]
153. Miyamoto, R.; Kitagawa, D.; Kobatake, S. Fatigue resistance of photochromic Diarylethene in the presence of cyclodextrins with different pore sizes. *Bull. Chem. Soc. Jpn.* **2022**, *95*, 639–645. [CrossRef]
154. Masai, H. Controlling excited-state dynamics and chemical reactivities of platinum acetylide complexes via self-threading ligands with permethylated α-cyclodextrin. *Bull. Chem. Soc. Jpn.* **2023**, *96*, 1196–1205. [CrossRef]
155. Kadokawa, J. A mini-review: Fabrication of polysaccharide composite materials based on self-assembled chitin nanofibers. *Materials* **2024**, *17*, 1898. [CrossRef] [PubMed]
156. Li, C.; Iqbal, M.; Lin, J.; Luo, X.; Jiang, B.; Malgras, V.; Wu, K.C.-W.; Kim, K.; Yamauchi, Y. Electrochemical deposition: An advanced approach for templated synthesis of nanoporous metal architectures. *Acc. Chem. Res.* **2018**, *51*, 1764–1773. [CrossRef] [PubMed]
157. Kamiyama, A.; Kubota, K.; Igarashi, D.; Youn, Y.; Tateyama, Y.; Ando, H.; Gotoh, K.; Komaba, S. MgO-template synthesis of extremely high capacity hard carbon for Na-ion battery. *Angew. Chem. Int. Ed.* **2021**, *60*, 5114–5120. [CrossRef] [PubMed]
158. Pan, Z.-Z.; Lv, W.; Yang, Q.-H.; Nishihara, H. Aligned macroporous monoliths by ice-templating. *Bull. Chem. Soc. Jpn.* **2022**, *95*, 611–620. [CrossRef]
159. Song, Y.; Song, X.; Wang, X.; Bai, J.; Cheng, F.; Lin, C.; Wang, X.; Zhang, H.; Sun, J.; Zhao, T.; et al. Two-dimensional metal–organic framework superstructures from ice-templated self-assembly. *J. Am. Chem. Soc.* **2022**, *144*, 17457–17467. [CrossRef]
160. Matsune, H.; Ikemizu, R.; Shiomori, K.; Muraoka, E.; Yamamoto, T.; Kishida, M. Colloidal trehalose nanoparticles: Sacrifice templates for hollow silica nanospheres. *Bull. Chem. Soc. Jpn.* **2023**, *96*, 813–815. [CrossRef]
161. Larasati, L.; Lestari, W.W.; Firdaus, M. Dual-action Pt(IV) prodrugs and targeted delivery in metal-organic frameworks: Overcoming cisplatin resistance and improving anticancer activity. *Bull. Chem. Soc. Jpn.* **2022**, *95*, 1561–1577. [CrossRef]
162. Dai, S.; Kajiwara, T.; Ikeda, M.; Romero-Muñiz, I.; Patriarche, G.; Platero-Prats, A.E.; Vimont, A.; Daturi, M.; Tissot, A.; Xu, Q.; et al. Ultrasmall copper nanoclusters in zirconium metal-organic frameworks for the photoreduction of CO_2. *Angew. Chem. Int. Ed.* **2022**, *61*, e202211848. [CrossRef]
163. Horike, S. Glass and liquid chemistry of coordination polymers and MOFs. *Bull. Chem. Soc. Jpn.* **2023**, *96*, 887–898. [CrossRef]
164. Mori, K.; Fujita, T.; Hata, H.; Kim, H.-J.; Nakano, T.; Yamashita, H. Surface chemical engineering of a metal 3D-printed flow reactor using a metal–organic framework for liquid-phase catalytic H_2 production from hydrogen storage materials. *ACS Appl. Mater. Interfaces* **2023**, *15*, 51079–51088. [CrossRef]
165. Li, J.; Yu, Z.; Zhang, J.; Liu, C.; Zhang, Q.; Shi, H.; Wu, D. Rapid, massive, and green synthesis of polyoxometalate-based metal–organic frameworks to fabricate POMOF/PAN nanofiber membranes for selective filtration of cationic dyes. *Molecules* **2024**, *29*, 1493. [CrossRef]
166. EL-Mahdy, A.F.M.; Omr, H.A.E.; ALOthman, Z.A.; Lee, H. Design and synthesis of metal-free ethene-based covalent organic framework photocatalysts for efficient, selective, and long-term stable CO_2 conversion into methane. *J. Colloid Interface Sci.* **2023**, *633*, 775–785. [CrossRef]
167. Sun, K.; Silveira, O.J.; Ma, Y.; Hasegawa, Y.; Matsumoto, M.; Kera, S.; Krejčí, O.; Foster, A.S.; Kawai, S. On-surface synthesis of disilabenzene-bridged covalent organic frameworks. *Nat. Chem.* **2023**, *15*, 136–142. [CrossRef] [PubMed]
168. Xiao, J.; Chen, J.; Liu, J.; Ihara, H.; Qiu, H. Synthesis strategies of covalent organic frameworks: An overview from nonconventional heating methods and reaction media. *Green Energy Environ.* **2023**, *8*, 1596–1618. [CrossRef]
169. Ma, B.; Zhong, L.; Huang, S.; Xiao, M.; Wang, S.; Han, D.; Meng, Y. Covalent organic framework enhanced solid polymer electrolyte for lithium metal batteries. *Molecules* **2024**, *29*, 1759. [CrossRef]
170. Hamieh, T. London dispersive and Lewis acid-base surface energy of 2D single-crystalline and polycrystalline covalent organic frameworks. *Crystals* **2024**, *14*, 148. [CrossRef]

171. Crudden, C.; Horton, J.; Ebralidze, I.; Zenkina, O.V.; McLean, A.B.; Drevniok, B.; She, Z.; Kraatz, H.-B.; Mosey, N.J.; Seki, T.; et al. Ultra stable self-assembled monolayers of N-heterocyclic carbenes on gold. *Nat. Chem.* **2014**, *6*, 409–414. [CrossRef] [PubMed]
172. Kawasaki, Y.; Nakagawa, M.; Ito, T.; Imura, Y.; Wang, K.-H.; Kawai, T. Chiral transcription from chiral Au nanowires to self-assembled monolayers of achiral azobenzene derivatives. *Bull. Chem. Soc. Jpn.* **2022**, *95*, 1006–1010. [CrossRef]
173. Das, S.; Ishiwari, F.; Shoji, Y.; Fukushima, T.; Zharnikov, M. Triptycene-based self-assembled monolayer as a template for successive click reactions. *J. Phys. Chem. C* **2023**, *127*, 5178–5185. [CrossRef]
174. Nakano, M.; Matsui, H.; Nakagawa, S.; You, J.; Shahiduzzaman, M.; Karakawa, M.; Taima, T. Control of the resistive switching voltage and reduction of the high-resistive-state current of zinc oxide by self-assembled monolayers. *Chem. Commun.* **2023**, *59*, 5761–5764. [CrossRef] [PubMed]
175. Wang, J.; Gadenne, V.; Patrone, L.; Raimundo, J.-M. Self-assembled monolayers of push–pull chromophores as active layers and their applications. *Molecules* **2024**, *29*, 559. [CrossRef]
176. Ariga, K.; Yamauchi, Y.; Mori, T.; Hill, J.P. 25th Anniversary article: What can be done with the Langmuir-Blodgett method? Recent developments and its critical role in materials science. *Adv. Mater.* **2013**, *25*, 6477–6512. [CrossRef] [PubMed]
177. Adachi, J.; Naito, M.; Sugiura, S.; Le, N.H.-T.; Nishimura, S.; Huang, S.; Suzuki, S.; Kawamorita, S.; Komiya, N.; Hill, J.P.; et al. Coordination amphiphile: Design of planar-coordinated platinum complexes for monolayer formation at an air-water interface based on ligand characteristics and molecular topology. *Bull. Chem. Soc. Jpn.* **2022**, *95*, 889–897. [CrossRef]
178. Negi, S.; Hamori, M.; Kitagishi, H.; Kano, K. Highly ordered monolayers of an optically active amphiphilic Pyrene derivative at the air–water interface. *Bull. Chem. Soc. Jpn.* **2022**, *95*, 1537–1545. [CrossRef]
179. Oliveira, O.N., Jr.; Caseli, L.; Ariga, K. The past and the future of Langmuir and Langmuir–Blodgett films. *Chem. Rev.* **2022**, *122*, 6459–6513. [CrossRef]
180. Negi, S.; Hamori, M.; Kubo, Y.; Kitagishi, H.; Kano, K. Monolayer formation and chiral recognition of binaphthyl amphiphiles at the air–water interface. *Bull. Chem. Soc. Jpn.* **2023**, *96*, 48–56. [CrossRef]
181. Tang, Z.; Wang, Y.; Podsiadlo, P.; Kotov, N. Biomedical applications of layer-by-layer assembly: From biomimetics to tissue engineering. *Adv. Mater.* **2006**, *18*, 3203–3224. [CrossRef]
182. Qiu, X.; Li, Z.; Li, X.; Zhang, Z. Flame retardant coatings prepared using layer by layer assembly: A review. *Chem. Eng. J.* **2018**, *334*, 108–122. [CrossRef]
183. Guzmán, E.; Ortega, F.; Rubio, R.G. Layer-by-layer nanoassemblies for vaccination purposes. *Pharmaceutics* **2023**, *15*, 1449. [CrossRef]
184. Jin, Y.; Zhang, S. Adenosine encapsulation and characterization through layer-by-layer assembly of hydroxypropyl-β-cyclodextrin and whey protein isolate as wall materials. *Molecules* **2024**, *29*, 2046. [CrossRef] [PubMed]
185. Pereira, J.M.; Mendes, J.P.; Dias, B.; Almeida, J.M.M.M.d.; Coelho, L.C.C. Optical pH sensor based on a long-period fiber grating coated with a polymeric Layer-by-layer electrostatic self-assembled nanofilm. *Sensors* **2024**, *24*, 1662. [CrossRef]
186. Ariga, K.; Li, J.; Fei, J.; Ji, Q.; Hill, J.P. Nanoarchitectonics for dynamic functional materials from atomic-/molecular-level manipulation to macroscopic action. *Adv. Mater.* **2016**, *28*, 1251–1286. [CrossRef]
187. Ariga, K.; Jia, X.; Song, J.; Hill, J.P.; Leong, D.T.; Jia, Y.; Li, J. Nanoarchitectonics beyond Self-Assembly: Challenges to Create Bio-Like Hierarchic Organization. *Angew. Chem. Int. Ed.* **2020**, *59*, 15424–15446. [CrossRef]
188. Ariga, K.; Nishikawa, M.; Mori, T.; Takeya, J.; Shrestha, L.K.; Hill, J.P. Self-assembly as a key player for materials nanoarchitectonics. *Sci. Technol. Adv. Mater.* **2019**, *20*, 51–95. [CrossRef]
189. Aono, M.; Ariga, K. The way to nanoarchitectonics and the way of nanoarchitectonics. *Adv. Mater.* **2016**, *28*, 989–992. [CrossRef]
190. Ariga, K. Nanoarchitectonics: A navigator from materials to life. *Mater. Chem. Front.* **2017**, *1*, 208–211. [CrossRef]
191. Ariga, K.; Yamauchi, Y. Nanoarchitectonics from atom to life. *Chem. Asian J.* **2020**, *15*, 718–728. [CrossRef] [PubMed]
192. Nakanishi, W.; Minami, K.; Shrestha, L.K.; Ji, Q.; Hill, J.P.; Ariga, K. Bioactive nanocarbon assemblies: Nanoarchitectonics and applications. *Nano Today* **2014**, *9*, 378–394. [CrossRef]
193. Nguyen, N.T.K.; Lebastard, C.; Wilmet, M.; Dumait, N.; Renaud, A.; Cordier, S.; Ohashi, N.; Uchikoshi, T.; Fabien Grasset, F. A review on functional nanoarchitectonics nanocomposites based on octahedral metal atom clusters (Nb_6, Mo_6, Ta_6, W_6, Re_6): Inorganic 0D and 2D powders and films. *Sci. Technol. Adv. Mater.* **2022**, *23*, 547–578. [CrossRef] [PubMed]
194. Huang, L.; Yang, J.; Asakura, Y.; Shuai, Q.; Yamauchi, Y. Nanoarchitectonics of hollow covalent organic frameworks: Synthesis and applications. *ACS Nano* **2023**, *17*, 8918–8934. [CrossRef] [PubMed]
195. Guan, X.; Li, Z.; Geng, X.; Lei, Z.; Karakoti, A.; Wu, T.; Kumar, P.; Yi, J.; Vinu, A. Emerging trends of carbon-based quantum dots: Nanoarchitectonics and applications. *Small* **2023**, *19*, 2207181. [CrossRef]
196. Han, M.; Kani, K.; Na, J.; Kim, J.; Bando, Y.; Ahamad, T.; Alshehri, S.M.; Yamauchi, Y. Retrospect and prospect: Nanoarchitectonics of platinum-group-metal-based materials. *Adv. Funct. Mater.* **2023**, *33*, 2301831. [CrossRef]
197. Ruiz-Hitzky, E.; Ruiz-Garci, C. MXenes vs. clays: Emerging and traditional 2D layered nanoarchitectonics. *Nanoscale* **2023**, *15*, 18959–18979. [CrossRef] [PubMed]
198. Kao, Y.-C.; Lin, J.-Y.; Chen, W.-C.; Gamal Mohamed, M.; Huang, C.-F.; Chen, J.-H.; Kuo, S.-W. High-thermal stable epoxy resin through blending nanoarchitectonics with double-decker-shaped polyhedral silsesquioxane-functionalized benzoxazine derivatives. *Polymers* **2024**, *16*, 112. [CrossRef] [PubMed]
199. Ramanathan, M.; Shrestha, L.K.; Mori, T.; Ji, Q.; Hill, J.P.; Ariga, K. Amphiphile nanoarchitectonics: From basic physical chemistry to advanced applications. *Phys. Chem. Chem. Phys.* **2013**, *15*, 10580–10611. [CrossRef]

200. Ariga, K.; Shionoya, M. Nanoarchitectonics for coordination asymmetry and related chemistry. *Bull. Chem. Soc. Jpn.* **2021**, *94*, 839–859. [CrossRef]
201. Gupta, D.; Varghese, B.S.; Suresh, M.; Panwar, C.; Gupta, T.K. Nanoarchitectonics: Functional nanomaterials and nanostructures—A review. *J. Nanopart. Res.* **2022**, *24*, 196. [CrossRef]
202. Cao, L.; Huang, Y.; Parakhonskiy, B.; Skirtach, A.G. Nanoarchitectonics beyond perfect order—Not quite perfect but quite useful. *Nanoscale* **2022**, *14*, 15964–16002. [CrossRef]
203. Pahal, S.; Boranna, R.; Tripathy, A.; Goudar, V.S.; Veetil, V.T.; Kurapati, R.; Prashanth, G.R.; Vemula, P.K. Nanoarchitectonics for free-standing polyelectrolyte multilayers films: Exploring the flipped surfaces. *ChemNanoMat* **2023**, *9*, e202200462. [CrossRef]
204. Datta, K.K.R. Exploringthe self-cleaning facets of fluorinated graphene nanoarchitectonics: Progress and perspectives. *ChemNanoMat* **2023**, *9*, e202300135. [CrossRef]
205. Jadhav, R.W.; Nadimetla, D.N.; Gawade, V.K.; Jones, L.A.; Bhosale, S.V. Mimicking the natural world with nanoarchitectonics for self-assembled superstructures. *Chem. Rec.* **2023**, *23*, e202200180. [CrossRef]
206. Nayak, A.; Unayama, S.; Tai, S.; Tsuruoka, T.; Waser, R.; Aono, M.; Valov, I.; Hasegawa, T. Nanoarchitectonics for controlling the number of dopant atoms in solid electrolyte nanodots. *Adv. Mater.* **2018**, *30*, 1703261. [CrossRef]
207. Eguchi, M.; Nugraha, A.S.; Rowan, A.E.; Shapter, J.; Yamauchi, Y. Adsorchromism: Molecular nanoarchitectonics at 2D nanosheets—Old chemistry for advanced chromism. *Adv. Sci.* **2021**, *8*, 2100539. [CrossRef]
208. Yao, B.; Sun, H.; He, Y.; Wang, S.; Liu, X. Recent advances in the photoreactions triggered by porphyrin-based triplet–triplet annihilation upconversion systems: Molecular innovations and nanoarchitectonics. *Int. J. Mol. Sci.* **2022**, *23*, 8041. [CrossRef]
209. Hikichi, R.; Tokura, Y.; Igarashi, Y.; Imai, H.; Oaki, Y. Fluorine-free substrate-independent superhydrophobic Coatings by nanoarchitectonics of polydispersed 2D materials. *Bull. Chem. Soc. Jpn.* **2023**, *96*, 766–774. [CrossRef]
210. Parbat, D.; Jana, N.; Dhar, M.; Manna, U. Reactive multilayer coating as versatile nanoarchitectonics for customizing various bioinspired liquid wettabilities. *ACS Appl. Mater. Interfaces* **2023**, *15*, 25232–25247. [CrossRef]
211. Li, M.; Wu, Z.; Tian, Y.; Pan, F.; Gould, T.; Zhang, S. Nanoarchitectonics of two-dimensional electrochromic Materials: Achievements and future challenges. *Adv. Mater. Technol.* **2023**, *8*, 2200917. [CrossRef]
212. Zhang, X.; Yang, P. $CsPbX_3$ (X = Cl, Br, and I) Nanocrystals in substrates toward stable photoluminescence: Nanoarchitectonics, properties, and applications. *Langmuir* **2023**, *39*, 11188–11212. [CrossRef]
213. Komiyama, M.; Yoshimoto, K.; Sisido, M.; Ariga, K. Chemistry can make strict and fuzzy controls for bio-systems: DNA nanoarchitectonics and cell-macromolecular nanoarchitectonics. *Bull. Chem. Soc. Jpn.* **2017**, *90*, 967–1004. [CrossRef]
214. Jia, Y.; Yan, X.; Li, J. Schiff base mediated dipeptide assembly toward nanoarchitectonics. *Angew. Chem. Int. Ed.* **2022**, *61*, e202207752. [CrossRef]
215. Shen, X.; Song, J.; Sevencan, C.; Leong, D.T.; Ariga, K. Bio-interactive nanoarchitectonics with two-dimensional materials and environments. *Sci. Technol. Adv. Mater.* **2022**, *23*, 199–224. [CrossRef]
216. Chang, R.; Zhao, L.; Xing, R.; Li, J.; Yan, X. Functional chromopeptide nanoarchitectonics: Molecular design, self-assembly and biological applications. *Chem. Soc. Rev.* **2023**, *52*, 2688–2712. [CrossRef]
217. Wu, M.; Liu, J.; Wang, X.; Zeng, H. Recent advances in antimicrobial surfaces via tunable molecular interactions: Nanoarchitectonics and bioengineering applications. *Curr. Opin. Colloid Interface Sci.* **2023**, *66*, 101707. [CrossRef]
218. Agamendran, N.; Uddin, M.; Yesupatham, M.S.; Shanmugam, M.; Augustin, A.; Kundu, T.; Kandasamy, R.; Sasaki, K.; Sekar, K. Nanoarchitectonics design strategy of metal–organic framework and bio-metal–organic framework composites for advanced wastewater treatment through adsorption. *Langmuir* **2024**, *40*, 3320–3334. [CrossRef]
219. Javed, A.; Kong, N.; Mathesh, M.; Duan, W.; Yang, W. Nanoarchitectonics-based electrochemical aptasensors for highly efficient exosome detection. *Sci. Technol. Adv. Mater.* **2024**, *25*, 2345041. [CrossRef]
220. Zhang, X.; Matras-Postolek, K.; Yang, P.; Jiang, S.P. Z-scheme WOx/Cu-g-C_3N_4 heterojunction nanoarchitectonics with promoted charge separation and transfer towards efficient full solar-spectrum photocatalysis. *J. Colloid Interface Sci.* **2023**, *636*, 646–656. [CrossRef]
221. Sadanandan, A.M.; Yang, J.-H.; Devtade, V.; Singh, G.; Dharmarajan, N.P.; Fawaz, M.; Lee, J.M.; Tavakkoli, E.; Jeon, C.-H.; Kumar, P.; et al. Carbon nitride based nanoarchitectonics for nature-inspired photocatalytic CO_2 reduction. *Prog. Mater. Sci.* **2024**, *142*, 101242. [CrossRef]
222. Ma, Y.; Xu, J.; Li, Z.; Shang, Y.; Li, Q. Nanoarchitectonics of $CoMoO_4$/NiS catalyst with starry flower morphology for carrier transport path investigation with advanced and photocatalytic hydrogen evolution performance. *Int. J. Hydrogen Energy* **2024**, *59*, 937–946. [CrossRef]
223. Thangamani, K.S.; Suba, V.; Radha, V.P.; Pradheesh, G.; Prabakaran, M. Investigation on nanoarchitectonics of PJBAC/TiO_2 for photocatalytic and antimicrobial performance. *J. Water Chem. Technol.* **2024**, *46*, 132–148. [CrossRef]
224. Wang, W.; Zhang, G.; Wang, Q.; Meng, F.; Jia, H.; Jiang, W.; Ji, Q. Hybrid nanoarchitectonics of TiO_2/aramid nanofiber membranes with softness and durability for photocatalytic dye degradation. *Chin. Chem. Lett.* **2024**, *35*, 109193. [CrossRef]
225. Yuan, Y.; He, J.; Dong, W.; Xie, X.; Liu, Y.; Wang, Z. Nanoarchitectonics of CuO/α-Fe_2O_3/$BiVO_4$ photocatalysts with double heterojunctions on PVDF membranes: Investigating sulfadiazine removal and antifouling properties. *Chem. Eng. J.* **2024**, *487*, 150445. [CrossRef]

226. Guan, X.; Zhang, X.; Li, Z.; Deshpande, S.; Fawaz, M.; Dharmarajan, N.P.; Lin, C.-H.; Lei, Z.; Hu, L.; Huang, J.-K.; et al. Sulfoxide-functional nanoarchitectonics of mesoporous sulfur-doped $C3N_5$ for photocatalytic hydrogen evolution. *Chem. Mater.* **2024**, *36*, 4511–4520. [CrossRef]
227. Chen, G.; Sciortino, F.; Ariga, K. Atomic Nanoarchitectonics for catalysis. *Adv. Mater. Interfaces* **2021**, *8*, 2001395. [CrossRef]
228. Chen, G.; Singh, S.K.; Takeyasu, K.; Hill, J.P.; Nakamura, J.; Ariga, K. Versatile nanoarchitectonics of Pt with morphology control of oxygen reduction reaction catalysts. *Sci. Technol. Adv. Mater.* **2022**, *23*, 413–423. [CrossRef]
229. Huang, C.; Qin, P.; Luo, Y.; Ruan, Q.; Liu, L.; Wu, Y.; Li, Q.; Xu, Y.; Liu, R.; Chu, P.K. Recent progress and perspective of cobalt-based catalysts for water splitting: Design and nanoarchitectonics. *Mater. Today Energy* **2022**, *23*, 100911. [CrossRef]
230. Sharma, D.; Choudhary, P.; Kumar, S.; Krishnan, V. Transition metal phosphide nanoarchitectonics for versatile organic catalysis. *Small* **2023**, *19*, 2207053. [CrossRef] [PubMed]
231. Choudhary, P.; Chauhan, S.S.; Sharma, D.; Kumar, S.; Krishnan, V. Nanoarchitectonics of sulfonated boron nitride for catalytic synthesis of aromatic nitriles under mild conditions. *Chem. Eng. J.* **2023**, *475*, 146055. [CrossRef]
232. Zhang, X.; Yang, P. g-C_3N_4 Nanosheet nanoarchitectonics: H_2 Generation and CO_2 reduction. *ChemNanoMat* **2023**, *9*, e202300041. [CrossRef]
233. Jiang, B.; Guo, Y.; Sun, F.; Wang, S.; Kang, Y.; Xu, X.; Zhao, J.; You, J.; Eguchi, M.; Yamauchi, Y.; et al. Nanoarchitectonics of metallene materials for electrocatalysis. *ACS Nano* **2023**, *17*, 13017–13043. [CrossRef]
234. Ishihara, S.; Labuta, J.; Rossom, W.V.; Ishikawa, D.; Minami, K.; Hill, J.P.; Ariga, K. Porphyrin-based sensor nanoarchitectonics in diverse physical detection modes. *Phys. Chem. Chem. Phys.* **2014**, *16*, 9713–9746. [CrossRef]
235. Komiyama, M.; Mori, T.; Ariga, K. Molecular Imprinting: Materials nanoarchitectonics with molecular information. *Bull. Chem. Soc. Jpn.* **2018**, *91*, 1075–1111. [CrossRef]
236. Yang, Y.; Du, X.; Jiang, D.; Shan, X.; Wang, W.; Shiigi, H.; Chen, Z. Photo-assisted Zn-air battery promoted self-powered sensor for selective and sensitive detection of antioxidant gallic acid based on Z-scheme nanoarchitectonics with heterojunction AgBr/$CuBi_2O_4$. *Sens. Actuat. B Chem.* **2023**, *393*, 134302. [CrossRef]
237. Xu, Y.; Yan, B.; Lai, C.; Wang, M.; Cao, Y.; Tu, J.; Chen, D.; Liu, Y.; Wu, Q. High-performance Vo-ZnO/ZnS benefiting nanoarchitectonics from the synergism between defect engineering and surface engineering for photoelectrochemical glucose sensors. *RSC Adv.* **2023**, *13*, 19782–19788. [CrossRef]
238. Vaghasiya, J.V.; Mayorga-Martinez, C.C.; Pumera, M. Wearable sensors for telehealth based on emerging materials and nanoarchitectonics. *npj Flex. Electron.* **2023**, *7*, 26. [CrossRef]
239. Wang, C.; Cui, Z.; Zhu, Y.; Liu, X.; Wang, L.; Wang, L.J. Nanoarchitectonics of high-sensitivity humidity sensors based on graphene oxide films for respiratory monitoring. *Diam. Relat. Mater.* **2024**, *144*, 110970. [CrossRef]
240. Sasaki, Y.; Lyu, X.; Kawashima, T.; Zhang, Y.; Ohshiro, K.; Okabe, K.; Tsuchiya, K.; Minami, T. Nanoarchitectonics of highly dispersed polythiophene on paper for accurate quantitative detection of metal ions. *RSC Adv.* **2024**, *14*, 5159–5166. [CrossRef]
241. Liu, J.; Wang, R.; Zhou, H.; Mathesh, M.; Dubey, M.; Zhang, W.; Wang, B.; Yang, W. Nucleic acid isothermal amplification-based soft nanoarchitectonics as an emerging electrochemical biosensing platform. *Nanoscale* **2022**, *14*, 10286–10298. [CrossRef]
242. Kim, S.K.; Lee, J.U.; Jeon, M.J.; Kim, S.K.; Hwang, S.-H.; Honge, M.E.; Sim, S.J. Bio-conjugated nanoarchitectonics with dual-labeled nanoparticles for a colorimetric and fluorescent dual-mode serological lateral flow immunoassay sensor in detection of SARS-CoV-2 in clinical samples. *RSC Adv.* **2023**, *13*, 27225–27232. [CrossRef] [PubMed]
243. Geetha, B.; Deepa, P.N. Nanoarchitectonics of a new rGO/poly(p-aminobenzoic acid) (pPABA)-based molecularly imprinted polymer electrode for detecting ascorbic acid, uric acid and glucose. *J. Solid State Electrochem.* **2024**, *28*, 357–375.
244. Huanga, P.; Wu, W.; Li, M.; Li, Z.; Pan, L.; Ahamad, T.; Alshehri, S.M.; Bando, Y.; Yamauchi, Y.; Xu, X. Metal-organic framework-based nanoarchitectonics: A promising material platform for electrochemical detection of organophosphorus pesticides. *Coord. Chem. Rev.* **2024**, *501*, 215534. [CrossRef]
245. Kathiravan, A.; Premkumar, S.; Jhons, M.A. Nanoarchitectonics of *Melia dubia* flowers to fluorescent carbon dots and its Ferritin sensing. *Colloid Surf. A Physicochem. Eng. Asp.* **2024**, *681*, 132824. [CrossRef]
246. Mukherjee, S.; Mukherjee, A.; Bytesnikova, Z.; Ashrafi, A.M.; Richtera, L.; Adam, V. 2D graphene-based advanced nanoarchitectonics for electrochemical biosensors: Applications in cancer biomarker detection. *Biosens. Bioelectron.* **2024**, *250*, 116050. [CrossRef]
247. Geravand, M.; Erfani, Y.; Nematpour, N.; Khosravani, M.; Rahimnia, R.; Adabi, M. Nanoarchitectonics of aptamer-based electrochemical biosensor utilizing electerospun carbon nanofibers and gold nanoparticles for Acinetobacter baumannii detection. *Microchem. J.* **2024**, *200*, 110437. [CrossRef]
248. Giussi, J.M.; Cortez, M.L.; Marmisollé, W.A.; Azzaroni, O. Practical use of polymer brushes in sustainable energy applications: Interfacial nanoarchitectonics for high-efficiency devices. *Chem. Soc. Rev.* **2019**, *48*, 814–849. [CrossRef]
249. Tsuchiya, T.; Nakayama, T.; Ariga, K. Nanoarchitectonics Intelligence with atomic switch and neuromorphic network system. *Appl. Phys. Express* **2022**, *15*, 100101. [CrossRef]
250. Azzaroni, O.; Piccinini, E.; Fenoy, G.; Marmisollé, W.; Ariga, K. Field-effect transistors engineered via solution-based layer-by-layer nanoarchitectonics. *Nanotechnology* **2023**, *34*, 472001. [CrossRef]
251. Zhou, F.; Zhao, Y.; Fu, F.; Liu, L.; Luo, Z. Thickness nanoarchitectonics with edge-enhanced raman, polarization Raman, optoelectronic properties of GaS nanosheets devices. *Crystals* **2023**, *13*, 1506. [CrossRef]

252. Baek, S.; Kim, S.; Han, S.A.; Kim, Y.H.; Kim, S.; Kim, J.H. Synthesis strategies and nanoarchitectonics for high-performance transition metal qichalcogenide thin film field-effect transistors. *ChemNanoMat* **2023**, *9*, e202300104. [CrossRef]
253. Xie, C.; Zhang, X.; Shi, W.; Yang, P. Highly luminescent $CsPbX_3$@MIL-53(Al) nanoarchitectonics with anomalous stability towards flexible emitting films. *J. Alloys Compd.* **2024**, *986*, 174132. [CrossRef]
254. Zhao, H.; Li, J.; Sun, W.; He, L.; Li, X.; Jia, X.; Qin, D. Dye-based nanoarchitectonics for the effective bandgap and stability of blue phosphorescent organic light-emitting diodes. *Appl. Phys. A* **2024**, *130*, 53. [CrossRef]
255. Kim, M.; Firestein, K.L.; Fernando, J.F.S.; Xu, X.; Lim, H.; Golberg, D.V.; Na, J.; Kim, J.; Nara, H.; Tang, J.; et al. Strategic design of Fe and N co-doped hierarchically porous carbon as superior ORR catalyst: From the perspective of nanoarchitectonics. *Chem. Sci.* **2022**, *13*, 10836–10845. [CrossRef] [PubMed]
256. Thmaini, N.; Charradi, K.; Ahmed, Z.; Chtourou, R.; Aranda, P. Nanoarchitectonics of fibrous clays as fillers of improved proton-conducting membranes for fuel-cell applications. *Appl. Clay Sci.* **2023**, *242*, 107019. [CrossRef]
257. Ju, L.; Hao, G.; Meng, F.; Jiang, W.; Ji, Q. Nanoarchitectonics tuning for Fe/N-doped C_{60}-derived carbon electrocatalysts with enhanced ORR activity by oxygen plasma treatment on C_{60}. *J. Mater. Chem. A* **2023**, *11*, 25534–25544. [CrossRef]
258. Ravipati, M.; Badhulika, S. Solvothermal synthesis of hybrid nanoarchitectonics nickel-metal organic framework modified nickel foam as a bifunctional electrocatalyst for direct urea and nitrate fuel cell. *Adv. Powder Technol.* **2023**, *34*, 104087. [CrossRef]
259. Liang, H.; Zhu, X.; Chen, Y.; Cheng, J. Nanoarchitectonics of yttrium-doped barium cerate-based proton conductor electrolyte for solid oxide fuel cells. *Appl. Phys. A* **2024**, *130*, 168. [CrossRef]
260. Allwyn, N.; Gokulnath, S.; Sathish, M. In-situ nanoarchitectonics of Fe/Co LDH over cobalt-enriched N-doped carbon cookies as facile oxygen redox electrocatalysts for high-rate rechargeable zinc–air batteries. *ACS Appl. Mater. Interfaces* **2024**, *16*, 20360–20374. [CrossRef]
261. Su, Y.; Ding, X.; Yuan, J. Trimetallicnanoarchitectonics of FeCoNi catalyst with modulated spin polarization for enhanced oxygen reduction performance. *Int. J. Hydrogen Energy* **2024**, *55*, 893–903. [CrossRef]
262. Vuk, D.; Radovanović-Perić, F.; Mandić, V.; Lovrinčević, V.; Rath, T.; Panžić, I.; Le-Cunff, J. Synthesis and nanoarchitectonics of novel squaraine derivatives for organic photovoltaic devices. *Nanomaterials* **2022**, *12*, 1206. [CrossRef] [PubMed]
263. Marineau-Plante, G.; Qassab, M.; Schlachter, A.; Nos, M.; Durandetti, M.; Hardouin, J.; Lemouchi, C.; Loïc Le Pluart, L.L.; Harvey, P.D. Photoreductive electron transfers in nanoarchitectonics organization between a diketopyrrolopyroleplatinum(II)-containing organometallic polymer and various electron acceptors. *J. Inorg. Organomet. Polym.* **2022**, *32*, 1266–1276. [CrossRef]
264. Bogachuk, D.; Girard, J.; Tilala, S.; Martineau, D.; Narbey, S.; Verma, A.; Hinsch, A.; Kohlstädt, M.; Wagner, L. Nanoarchitectonics in fully printed perovskite solar cells with carbon-based electrodes. *Nanoscale* **2023**, *15*, 3130–3134. [CrossRef] [PubMed]
265. Lappi, T.; Cordier, S.; Gayfulin, Y.; Ababou-Girard, S.; Grasset, F.; Uchikoshi, T.; Naumov, N.G.; Renaud, A. Nanoarchitectonics of metal atom cluster-based building blocks applied to the engineering of photoelectrodes for solar cells. *Sol. RRL* **2023**, *7*, 2201037. [CrossRef]
266. Qiu, D.; Hou, P. Ferroelectricity-driven self-powered weak temperature and broadband light detection in $MoS_2/CuInP_2S_6/WSe_2$ van der Waals heterojunction nanoarchitectonics. *ACS Appl. Mater. Interfaces* **2023**, *15*, 59671–59680. [CrossRef] [PubMed]
267. Kim, D.; Lim, H.; Kim, S.H.; Lee, K.N.; You, J.; Ryu, D.Y.; Kim, J. Recent developments of polymer-based encapsulants and backsheets for stable and high-performance silicon photovoltaic modules: Materials nanoarchitectonics and mechanisms. *J. Mater. Chem. A* **2024**, *12*, 7452–7469. [CrossRef]
268. Abdulrhman, M.; Abdel-Aal, S.K.; Bain, C.A.; Raptis, D.; Bernal-Texca, F.; Wlodarczyk, K.L.; Hand, D.P.; Martorell, J.; Marques-Hueso, J. Nanoarchitectonics of lead-free 2D cobalt-based diammonium hybrid for perovskites solar cell applications. *Appl. Phys. A* **2024**, *130*, 426. [CrossRef]
269. Koralkar, N.; Mehta, S.; Upadhyay, A.; Patel, G.; Deshmukh, K. MOF-based nanoarchitectonics for lithium-ion batteries: A comprehensive review. *J. Inorg. Organomet. Polym.* **2024**, *34*, 903–929. [CrossRef]
270. Bahadur, R.; Singh, G.; Li, Z.; Singh, B.; Srivastava, R.; Sakamoto, Y.; Chang, S.; Murugavel, R.; Vinu, A. Hybrid nanoarchitectonics of ordered mesoporous C_{60}–BCN with high surface area for supercapacitors and lithium-ion batteries. *Carbon* **2024**, *216*, 118568. [CrossRef]
271. Kozhunova, E.Y.; Inozemtseva, A.I.; Nazarov, M.A.; Nikolenko, A.D.; Zhvanskaya, E.S.; Kiselyova, O.I.; Motyakin, M.V.; Kutyakov, S.V.; Pakhomov, A.A.; Itkis, D.M.; et al. Nanoarchitectonics and electrochemical properties of redox-active nanogels for redox flow battery electrolytes. *Electrochim. Acta* **2024**, *475*, 143534. [CrossRef]
272. Yu, L.; Chang, M.; Zhang, M.; Yang, Y.; Chen, K.; Jiang, T.; Shi, D.; Zhang, Q.; You, J. Nanoarchitectonics of 3D-networked bio-based binders for silicon anodes in lithium-ion batteries based on dynamic hydrogen bonding. *Sustain. Energy Fuels* **2024**, *8*, 843–851. [CrossRef]
273. Zhang, X.; Xu, Z.; Xie, J.; Lu, Y.; Liu, S.; Xu, X.; Tu, J.; Xu, B.; Zhao, X. Nanoarchitectonics for a long-life and robust Na-ion battery at low temperature with Prussian blue cathode and low-concentration electrolyte. *J. Energy Storage* **2024**, *80*, 110263. [CrossRef]
274. Hsu, C.-C.; Yu, Y.Z.; Wu, C.-H.; Lee, P.-Y.; Chen, H.-M.; Husain, S.; Kongvarhodom, C.; Hsiao, Y.-C.; Lin, L.-Y. Metal ratio and bimetal nanoarchitectonics of ammonia-based fluoride complex induced nickel hydroxide and manganese oxide composites as active materials of an energy storage device. *J. Energy Storage* **2024**, *80*, 110316. [CrossRef]
275. Jheng, Y.-S.; Lue, S.-J.J.; Cheng, K.-W. Nanoarchitectonics of ternary $Ni_xCo_{1-x}Se_2$ electrocatalysts on Ni-foams combined with Pt-loaded carbon clothes as the air-cathodes in Zn-air energy storage systems. *J. Taiwan Inst. Chem. Eng.* **2024**, *159*, 105451. [CrossRef]

276. Na, J.; Zheng, D.; Kim, J.; Gao, M.; Azhar, A.; Lin, J.; Yamauchi, Y. Material nanoarchitectonics of functional polymers and inorganic nanomaterials for smart supercapacitors. *Small* **2022**, *18*, 2102397. [CrossRef]
277. Qi, P.; Su, Y.; Yang, L.; Wang, J.; Jiang, M.; Sun, X.; Zhang, P.; Xiong, Y. Nanoarchitectonics of hierarchical porous carbon based on carbonization of heavy fraction of bio-oil and its supercapacitor performance. *J. Energy Storage* **2023**, *74*, 109398. [CrossRef]
278. Joseph, A.; Ramachandran, S.; Thomas, T. Ball milling nanoarchitectonics of nitrogen-doped Cr_2O_3 on thermally exfoliated. amorphous nanosheets for a high-performance supercapacitor. *ChemistrySelect* **2023**, *8*, e202300808. [CrossRef]
279. Vivekanand; Balaji, S.S.; Nasrin, K.; Sathish, M. Unveiled supercapacitive performance of Se-doped graphene nanoarchitectonics prepared via supercritical fluid technique. *ChemNanoMat* **2023**, *9*, e202300209. [CrossRef]
280. Dong, K.; Sun, Z.; Jing, G.; Wang, J.; Tang, B.; Zhao, N.; Kong, L.; Guo, F. Nanoarchitectonics of self-supporting porous carbon electrode with heteroatoms co-doped: For high-performance supercapacitors. *J. Energy Storage* **2024**, *85*, 111048. [CrossRef]
281. Wang, H.; Shi, H.; Gao, Z.; Cui, X. Growing-fruits-type nanoarchitectonics of nickel-vanadium layered double hydroxide on branches of nitrogen-rich carbon nanotube for high performance supercapacitors. *J. Energy Storage* **2024**, *89*, 111745. [CrossRef]
282. Salunkhe, T.T.; Gurugubelli, T.R.; Bathula, B.; Thirumal, V.; Kim, J.; Yoo, K. Energy storage nanoarchitectonics of $La_2W_2O_9$ porous microspheres for advanced supercapacitive performance. *Mater. Chem. Phys.* **2024**, *315*, 128993. [CrossRef]
283. Khan, A.H.; Ghosh, S.; Pradhan, B.; Dalui, A.; Shrestha, L.K.; Acharya, S.; Ariga, K. Two-dimensional (2D) nanomaterials towards electrochemical nanoarchitectonics in energy-related applications. *Bull. Chem. Soc. Jpn.* **2017**, *90*, 627–648. [CrossRef]
284. Kim, J.; Kim, J.H.; Ariga, K. Redox-active polymers for energy storage nanoarchitectonics. *Joule* **2017**, *1*, 739–768. [CrossRef]
285. Feng, J.-C.; Xia, H. Application of nanoarchitectonics in moist-electric generation. *Beilstein J. Nanotechnol.* **2022**, *13*, 1185–1200. [CrossRef]
286. Geng, X.; Singh, G.; Sathish, C.I.; Li, Z.; Bahadur, R.; Liu, Y.; Li, S.; Yu, X.; Breese, M.; Yi, J.; et al. Biomass derived nanoarchitectonics of porous carbon with tunable oxygen functionalities and hierarchical structures and their superior performance in CO_2 adsorption and energy storage. *Carbon* **2023**, *214*, 118347. [CrossRef]
287. Ali, S.M.; Kassim, H.; Alaizeri, Z.A.M.; Shahabuddin, M. Enhanced electrochemical performance of novel nanoarchitectonics tin selenide (SnSe/rGO) pseudocapacitive material for energy storage application. *J. Energy Storage* **2023**, *73*, 109163. [CrossRef]
288. Gupta, P.; Jaidka, S.; Singh, D.P. Quenching induced modified nanoarchitectonics in the dielectric and energy storage behavior of poly (vinylidene fluoride)/$Ba_{0.7}Sr_{0.3}TiO_3$ composites thick films. *Appl. Phys. A* **2024**, *130*, 279. [CrossRef]
289. Chahal, S.; Bhushan, R.; Kumari, P.; Guan, X.; Lee, J.M.; Ray, S.J.; Thakur, A.K.; Vinu, A.; Kumar, P. Microwave nanoarchitectonics of black phosphorene for energy storage. *Matter* **2024**, *7*, 237–254. [CrossRef]
290. Pham, T.-A.; Qamar, A.; Dinh, T.; Masud, N.K.; Rais-Zadeh, M.; Senesky, D.G.; Yamauchi, Y.; Nguyen, N.-T.; Phan, H.-P. Nanoarchitectonics for wide bandgap semiconductor nanowires: Toward the next generation of nanoelectromechanical systems for environmental monitoring. *Adv. Sci.* **2020**, *7*, 2001294. [CrossRef]
291. Ali, N.; Funmilayo, O.R.; Khan, A.; Ali, F.; Bilal, M.; Yang, Y.; Akhter, M.S.; Zhou, C.; Wenjie, Y.; Iqbal, H.M.N. Nanoarchitectonics: Porous hydrogel as bio-sorbent for effective remediation of hazardous contaminants. *J. Inorg. Organomet. Polym.* **2022**, *32*, 3301–3320. [CrossRef]
292. Nawaz, A.; Atif, M.; Naz, I.; Khan, A.; Naz, F.; Ali, N. Comparative robustness and sustainability of in-situ prepared antimony nanoarchitectonics in chitosan/synthesized carboxymethyl chitosan in environmental remediation perspective. *Int. J. Biol. Macromol.* **2023**, *235*, 123591. [CrossRef] [PubMed]
293. Barreca, D.; Maccato, C. Nanoarchitectonics of metal oxide materials for sustainable technologies and environmental applications. *CrystEngComm* **2023**, *25*, 3968–3987. [CrossRef]
294. Bhadra, B.N.; Shrestha, L.K.; Ariga, K. Porous carbon nanoarchitectonics for the environment: Detection and adsorption. *CrystEngComm* **2022**, *24*, 6804–6824. [CrossRef]
295. Akamatsu, M. Inner and interfacial environmental nanoarchitectonics of supramolecular assemblies formed by amphiphiles: From emergence to application. *J. Oleo Sci.* **2023**, *72*, 105–116. [CrossRef]
296. Kumar, A.; Choudhary, P.; Chhabra, T.; Kaur, H.; Kumar, A.; Qamar, M.; Krishnan, V. Frontier nanoarchitectonics of graphitic carbon nitride based plasmonic photocatalysts and photoelectrocatalysts for energy, environment and organic reactions. *Mater. Chem. Front.* **2023**, *7*, 1197–1247. [CrossRef]
297. Molla, M.R.; Levkin, P.A. Combinatorial approach to nanoarchitectonics for nonviral delivery of nucleic acids. *Adv. Mater.* **2016**, *28*, 1159–1175. [CrossRef]
298. Momekova, D.B.; Gugleva, V.E.; Petrov, P.D. Nanoarchitectonics of multifunctional niosomes for advanced drug delivery. *ACS Omega* **2021**, *6*, 33265–33273. [CrossRef] [PubMed]
299. Ferhan, A.R.; Park, S.; Park, H.; Tae, H.; Jackman, J.A.; Cho, N.-J. Lipid nanoparticle technologies for nucleic acid delivery: A nanoarchitectonics perspective. *Adv. Funct. Mater.* **2022**, *32*, 2203669. [CrossRef]
300. Mohanan, S.; Guan, X.; Liang, M.; Karakoti, A.; Vinu, A. Stimuli-responsive silica silanol conjugates: Strategic nanoarchitectonics in targeted drug delivery. *Small* **2023**, 2301113. [CrossRef]
301. Komiyama, M. Cyclodextrins as eminent constituents in nanoarchitectonics for drug delivery systems. *Beilstein J. Nanotechnol.* **2023**, *14*, 218–232. [CrossRef]
302. Tian, W.; Wang, C.; Chu, R.; Ge, H.; Sun, X.; Li, M. Injectable hydrogel nanoarchitectonics with near-infrared controlled drug delivery for in situ photothermal/endocrine synergistic endometriosis therapy. *Biomater. Res.* **2023**, *27*, 100. [CrossRef] [PubMed]

303. Reddy, Y.N.; De, A.; Paul, S.; Pujari, A.K.; Bhaumik, J. In Situ Nanoarchitectonics of a MOF hydrogel: A self-adhesive and pH-responsive smart platform for phototherapeutic delivery. *Biomacromolecules* **2023**, *24*, 1717–1730. [CrossRef] [PubMed]
304. Hu, W.; Shi, J.; Lv, W.; Jia, X.; Ariga, K. Regulation of stem cell fate and function by using bioactive materials with nanoarchitectonics for regenerative medicine. *Sci. Technol. Adv. Mater.* **2022**, *23*, 393–412. [CrossRef] [PubMed]
305. Jang, T.-S.; Park, S.J.; Lee, J.E.; Yang, J.; Park, S.-H.; Jun, M.B.G.; Kim, Y.W.; Aranas, C.; Choi, J.P.; Zou, Y.; et al. Topography-supported nanoarchitectonics of hybrid scaffold for systematically modulated bone regeneration and remodeling. *Adv. Funct. Mater.* **2022**, *32*, 2206863. [CrossRef]
306. Jia, X.; Chen, J.; Lv, W.; Li, H.; Ariga, K. Engineering dynamic and interactive biomaterials using material nanoarchitectonics for modulation of cellular behaviors. *Cell Rep. Phys. Sci.* **2023**, *4*, 101251. [CrossRef]
307. Li, B.; Huang, Y.; Bao, J.; Xu, Z.; Yan, X.; Zou, Q. Supramolecular nanoarchitectonics based on antagonist peptide self-assembly for treatment of liver fibrosis. *Small* **2023**, *19*, 2304675. [CrossRef] [PubMed]
308. Wang, Y.; Li, P.; Cao, S.; Liu, Y.; Gao, C. Nanoarchitectonics composite hydrogels with high toughness, mechanical strength, and self-healing capability for electrical actuators with programmable shape memory properties. *Nanoscale* **2023**, *15*, 18667–18677. [CrossRef] [PubMed]
309. Mendes de Almeida Junior, A.; Ferreira, A.S.; Camacho, S.A.; Gontijo Moreira, L.; de Toledo, K.A.; Oliveira, O.N., Jr.; Aoki, P.H.B. Enhancing Phototoxicity in Human Colorectal Tumor Cells through Nanoarchitectonics for Synergistic Photothermal and Photodynamic Therapies. *ACS Appl. Mater. Interfaces* **2024**, *16*, 23742–23751. [CrossRef]
310. Wang, Y.; Geng, Q.; Zhang, Y.; Adler-Abramovich, L.; Fan, X.; Mei, D.; Gazit, E.; Tao, K. Fmoc-diphenylalanine gelating nanoarchitectonics: A simplistic peptide self-assembly to meet complex applications. *J. Colloid Interface Sci.* **2023**, *636*, 113–133. [CrossRef]
311. Kumbhar, P.; Kolekar, K.; Khot, C.; Dabhole, S.; Salawi, A.; Sabei, F.Y.; Mohite, A.; Kole, K.; Mhatre, S.; Jha, N.K.; et al. Co-crystal nanoarchitectonics as an emerging strategy in attenuating cancer: Fundamentals and applications. *J. Control. Release* **2023**, *353*, 1150–1170. [CrossRef] [PubMed]
312. Song, J.; Kawakami, K.; Ariga, K. Nanoarchitectonics in combat against bacterial infection using molecular, interfacial, and material tools. *Curr. Opin. Colloid Interface Sci.* **2023**, *65*, 101702. [CrossRef]
313. Sutrisno, L.; Ariga, K. Pore-engineered nanoarchitectonics for cancer therapy. *NPG Asia Mater.* **2023**, *15*, 21. [CrossRef]
314. Duan, H.; Wang, F.; Xu, W.; Sheng, G.; Sun, Z.; Chu, H. Recentadvances in the nanoarchitectonics of metal–organic frameworks for light-activated tumor therapy. *Dalton Trans.* **2023**, *52*, 16085–16102. [CrossRef] [PubMed]
315. Zheng, C.; Wang, Z.; Xu, H.; Huang, H.; Tao, X.; Hu, Y.; He, Y.; Zhang, Z.; Huang, X. Redox-activatable magnetic nanoarchitectonics for self-enhanced tumor imaging and synergistic photothermal-chemodynamic therapy. *Small Methods* **2023**, *8*, 2301099. [CrossRef] [PubMed]
316. Meng, R.-Y.; Zhao, Y.; Xia, H.-Y.; Wang, S.-B.; Chen, A.-Z.; Kankala, R.K. 2D Architectures-transformed conformational nanoarchitectonics for light-augmented nanocatalytic chemodynamic and photothermal/photodynamic-based trimodal therapies. *ACS Mater. Lett.* **2024**, *6*, 1160–1177. [CrossRef]
317. Li, X.; Liu, Y.; Wu, L.; Zhao, J. Molecular nanoarchitectonics of natural photosensitizers and their derivatives nanostructures for improved photodynamic therapy. *ChemMedChem* **2024**, *19*, e202300599. [CrossRef] [PubMed]
318. Laughlin, R.B.; Pines, D. The theory of everything. *Proc. Natl. Acad. Sci. USA* **2000**, *97*, 28–31. [CrossRef] [PubMed]
319. Ariga, K.; Fakhrullin, R. Materials nanoarchitectonics from atom to living cell: A method for everything. *Bull. Chem. Soc. Jpn.* **2022**, *95*, 774–795. [CrossRef]
320. Ariga, K. Nanoarchitectonics: Method for everything in material science. *Bull. Chem. Soc. Jpn.* **2024**, *97*, uoad001. [CrossRef]
321. Ariga, K.; Kunitake, T. Molecular recognition at air−water and related interfaces: Complementary hydrogen bonding and multisite interaction. *Acc. Chem. Res.* **1998**, *31*, 371–378. [CrossRef]
322. Kurihara, K. Surface forces measurement for materials science. *Pure Appl. Chem.* **2019**, *91*, 707–716. [CrossRef]
323. Takada, K. Interfacial nanoarchitectonics for solid-state lithium batteries. *Langmuir* **2013**, *29*, 7538–7541. [CrossRef] [PubMed]
324. Ariga, K. Materials nanoarchitectonics in a two-dimensional world within a nanoscale distance from the liquid phase. *Nanoscale* **2022**, *14*, 10610–10629. [CrossRef] [PubMed]
325. Ariga, K. Don't forget Langmuir–Blodgett films 2020: Interfacial nanoarchitectonics with molecules, materials, and living objects. *Langmuir* **2020**, *36*, 7158–7180. [CrossRef] [PubMed]
326. Souza, A.L.; Osvaldo, N.; Oliveira, O.N. Dominant hydrophobic interactions with β-glucan in nanoarchitectonics with mixed Langmuir monolayers of cholesterol/dipalmitoyl phosphatidyl choline. *Biointerphases* **2022**, *17*, 031005. [CrossRef]
327. Martins, B.A.; Deffune, E.; Oliveira, O.N., Jr.; de Moraes, M.L. Penicillin-binding proteins (PBPs) determine antibiotic action in Langmuir monolayers as nanoarchitectonics mimetic membranes of methicillin-resistant Staphylococcus aureus. *Colloid Surf. B Biointerfaces* **2022**, *214*, 112447. [CrossRef] [PubMed]
328. Rydzek, G.; Ji, Q.; Li, M.; Schaaf, P.; Hill, J.P.; Boulmedais, F.; Ariga, K. Electrochemical nanoarchitectonics and layer-by-layer assembly: From basics to future. *Nano Today* **2015**, *10*, 138–167. [CrossRef]
329. Ariga, K.; Lvov, Y.; Decher, G. There is still plenty of room for layer-by-layer assembly for constructing nanoarchitectonics-based materials and devices. *Phys. Chem. Chem. Phys.* **2022**, *24*, 4097–4115. [CrossRef]
330. Ariga, K. Chemistry of materials nanoarchitectonics for two-dimensional films: Langmuir–Blodgett, layer-by-layer assembly, and newcomers. *Chem. Mater.* **2023**, *35*, 5233–5254. [CrossRef]

331. Ariga, K.; Song, J.; Kawakami, K. Layer-by-layer designer nanoarchitectonics for physical and chemical communications in functional materials. *Chem. Commun.* **2024**, *60*, 2152–2167. [CrossRef] [PubMed]
332. Miyazawa, K. Synthesis of fullerene nanowhiskers using the liquid–liquid interfacial precipitation method and their mechanical, electrical and superconducting properties. *Sci. Technol. Adv. Mater.* **2015**, *16*, 013502. [CrossRef] [PubMed]
333. Miyazawa, K.; Kuwasaki, Y.; Obayashi, A.; Kuwabara, M. C_{60} nanowhiskers formed by the liquid–liquid interfacial precipitation method. *J. Mater. Res.* **2002**, *17*, 83–88. [CrossRef]
334. Chang, C.-Y.; Wu, C.-E.; Chen, S.-Y.; Cui, C.; Cheng, Y.-J.; Hsu, C.-S.; Wang, Y.-L.; Li, Y. Enhanced performance and stability of a polymer solar cell by incorporation of vertically aligned, cross-linked fullerene nanorods. *Angew. Chem. Int. Ed.* **2011**, *50*, 9386–9390. [CrossRef]
335. Miyazawa, K.; Minato, J.; Yoshii, T.; Fujino, M.; Suga, T. Structural characterization of the fullerene nanotubes prepared by the liquid–liquid interfacial precipitation method. *J. Mater. Res.* **2005**, *20*, 688–695. [CrossRef]
336. Chen, G.; Shrestha, L.K.; Ariga, K. Zero-to-two nanoarchitectonics: Fabrication of two-dimensional materials from zero-dimensional fullerene. *Molecules* **2021**, *26*, 4636. [CrossRef]
337. Chen, G.; Bhadra, B.N.; Sutrisno, L.; Shrestha, L.K.; Ariga, K. Fullerene rosette: Two-dimensional interactive nanoarchitectonics and selective vapor sensing. *Int. J. Mol. Sci.* **2022**, *23*, 5454. [CrossRef]
338. Park, C.; Yoon, E.; Kawano, M.; Joo, T.; Choi, H.C. Self-crystallization of C_{70} cubes and remarkable enhancement of photoluminescence. *Angew. Chem. Int. Ed.* **2010**, *49*, 9670–9675. [CrossRef]
339. Bairi, P.; Minami, K.; Nakanishi, W.; Hill, J.; Ariga, K.; Shrestha, L. Hierarchically Structured Fullerene C_{70} Cube for Sensing Volatile Aromatic Solvent Vapors. *ACS Nano* **2016**, *10*, 6631–6637. [CrossRef]
340. Bairi, P.; Minami, K.; Hill, J.P.; Ariga, K.; Shrestha, L.K. Intentional Closing/Opening of "Hole-in-Cube" Fullerene Crystals with Microscopic Recognition Properties. *ACS Nano* **2017**, *11*, 7790–7796. [CrossRef]
341. Hsieh, C.-T.; Hsu, S.-h.; Maji, S.; Chahal, M.K.; Song, J.; Hill, J.P.; Ariga, K.; Shrestha, L.K. Post-assembly dimension-dependent face-selective etching of fullerene crystals. *Mater. Horiz.* **2020**, *7*, 787–795. [CrossRef]
342. Bairi, P.; Minami, K.; Hill, J.P.; Nakanishi, W.; Shrestha, L.K.; Liu, C.; Harano, K.; Nakamura, E.; Ariga, K. Supramolecular differentiation for constructing anisotropic fullerene nanostructures by time-programmed control of interfacial growth. *ACS Nano* **2016**, *10*, 8796–8802. [CrossRef]
343. Chen, G.; Sciortino, F.; Takeyasu, K.; Nakamura, J.; Hill, J.P.; Shrestha, L.K.; Ariga, K. Hollow spherical fullerene obtained by kinetically controlled liquid-liquid interfacial precipitation. *Chem. Asian J.* **2022**, *17*, e202200756. [CrossRef] [PubMed]
344. Banya, S.; Kumagawa, Y.; Izumoto, D.; Tanaka, M.; Kanbe, K.; Oku, T.; Akiyama, T. Fabrication and photoelectric conversion of densely packed C_{60}–ethylenediamine adduct microparticle films-modified electrode covered with electrochemically deposited polythiophene thin-films. *RSC Adv.* **2023**, *13*, 31244–31251. [CrossRef]
345. Takase, S.; Aritsu, T.; Sakamoto, Y.; Sakuno, Y.; Shimizu, Y. Preparation of highly conductive phthalocyaninato-cobalt iodide at the interface between aqueous KI solution and organic solvent and catalytic properties for electrochemical reduction of CO_2. *Bull. Chem. Soc. Jpn.* **2023**, *96*, 649–653. [CrossRef]
346. Kaneko, M.; Nakayama, T.; Seki, H.; Yamamoto, S.; Uemura, T.; Inoue, K.; Hadano, S.; Watanabe, S.; Niko, Y. Lipophilic nitrile N-oxide for catalyst-free surface modification of nanoemulsions as light-harvesting nanoantennas. *Bull. Chem. Soc. Jpn.* **2022**, *95*, 1760–1768. [CrossRef]
347. Sawayama, T.; Wang, Y.; Watanabe, T.; Takayanagi, M.; Yamamoto, T.; Hosono, N.; Uemura, T. Metal-organic frameworks for practical separation of cyclic and linear polymers. *Angew. Chem. Int. Ed.* **2021**, *60*, 11830–11834. [CrossRef] [PubMed]
348. Kioka, K.; Mizutani, N.; Hosono, N.; Uemura, T. Mixed metal–organic framework stationary phases for liquid chromatography. *ACS Nano* **2022**, *16*, 6771–6780. [CrossRef] [PubMed]
349. Ay, B.; Takano, R.; Ishida, T. Metal-organodiphosphonate chemistry: Hydrothermal syntheses and structures of two novel copper(II) coordination polymers with o-xylylenediphosphonic acid and 4,4′-bipyridine ligands. *Bull. Chem. Soc. Jpn.* **2023**, *96*, 1129–1138. [CrossRef]
350. Xu, X.; Eguchi, M.; Asakura, Y.; Pan, L.; Yamauchi, Y. Metal–organic framework derivatives for promoted capacitive deionization of oxygenated saline water. *Energy Environ. Sci.* **2023**, *16*, 1815–1820. [CrossRef]
351. Han, M.; Tashiro, S.; Shiraogawa, T.; Ehara, M.; Shionoya, M. Substrate-specific activation and long-range olefin migration catalysis at the Pd centers in a porous metal-macrocycle framework. *Bull. Chem. Soc. Jpn.* **2022**, *95*, 1303–1307. [CrossRef]
352. Geng, K.; He, T.; Liu, R.; Dalapati, S.; Tan, K.T.; Li, Z.; Tao, S.; Gong, Y.; Jiang, Q.; Jiang, D. Covalent organic frameworks: Design, synthesis, and functions. *Chem. Rev.* **2020**, *120*, 8814–8933. [CrossRef] [PubMed]
353. Stähler, C.; Grunenberg, L.; Terban, M.W.; Browne, W.R.; Doellerer, D.; Kathan, M.; Etter, M.; Bettina, V.; Lotsch, B.V.; Feringa, B.L.; et al. Light-driven molecular motors embedded in covalent organic frameworks. *Chem. Sci.* **2022**, *13*, 8253–8264. [CrossRef] [PubMed]
354. Ghosh, S.; Tsutsui, Y.; Kawaguchi, T.; Matsuda, W.; Nagano, S.; Suzuki, K.; Kaji, H.; Seki, S. Band-like transport of charge carriers in oriented two-dimensional conjugated covalent organic frameworks. *Chem. Mater.* **2022**, *34*, 736–745. [CrossRef]
355. Charles-Blin, Y.; Kondo, T.; Wu, Y.; Bandow, S.; Awaga, K. Salt-assisted pyrolysis of covalent organic framework for controlled active nitrogen functionalities for oxygen reduction reaction. *Bull. Chem. Soc. Jpn.* **2022**, *95*, 972–977. [CrossRef]
356. Yang, M.; Hanayama, H.; Fang, L.; Addicoat, M.A.; Guo, Y.; Graf, R.; Harano, K.; Kikkawa, J.; Jin, E.; Narita, A.; et al. Saturated linkers in two-dimensional covalent organic frameworks boost their luminescence. *J. Am. Chem. Soc.* **2023**, *145*, 14417–14426. [CrossRef] [PubMed]

357. Makiura, R.; Motoyama, S.; Umemura, Y.; Yamanaka, H.; Sakata, O.; Kitagawa, H. Surface nano-architecture of a metal–organic framework. *Nat. Mater.* **2010**, *9*, 565–571. [CrossRef] [PubMed]
358. Makiura, R. Creation of metal–organic framework nanosheets by the Langmuir-Blodgett technique. *Coord. Chem. Rev.* **2022**, *469*, 214650. [CrossRef]
359. Ohata, T.; Tachimoto, K.; Takeno, K.J.; Nomoto, A.; Watanabe, T.; Hirosawa, I.; Makiura, R. Influence of the solvent on the assembly of Ni_3(hexaiminotriphenylene)$_2$ metal–organic framework nanosheets at the air/liquid interface. *Bull. Chem. Soc. Jpn.* **2023**, *96*, 274–282. [CrossRef]
360. Moribe, S.; Takeda, Y.; Umehara, M.; Kikuta, H.; Ito, J.; Ma, J.; Yamada, Y.; Hirano, M. Spike current induction by photo-generated charge accumulation at the surface sites of porous porphyrinic zirconium metal-organic framework electrodes in photoelectrochemical cells. *Bull. Chem. Soc. Jpn.* **2023**, *96*, 321–327. [CrossRef]
361. Hong, J.; Liu, M.; Liu, Y.; Shang, S.; Wang, X.; Du, C.; Gao, W.; Hua, C.; Xu, H.; You, Z.; et al. Solid-liquid interfacial engineered large-area two-dimensional covalent organic framework films. *Angew. Chem. Int. Ed.* **2024**, *63*, e202317876. [CrossRef] [PubMed]
362. Zou, H.; Li, Q.; Zhang, R.; Xiong, Z.; Li, B.; Wang, J.; Wang, R.; Fang, Q.; Yang, H. Amphiphilic Covalent Organic Framework Nanoparticles for Pickering Emulsion Catalysis with Size Selectivity. *Angew. Chem. Int. Ed.* **2024**, *63*, e202314650. [CrossRef] [PubMed]
363. Du, J.; Sun, Q.; He, W.; Liu, L.; Song, Z.; Yao, A.; Ma, J.; Cao, D.; Hassan, S.U.; Guan, J.; et al. A 2D soft covalent organic framework membrane prepared via a molecular bridge. *Adv. Mater.* **2023**, *35*, 2300975. [CrossRef]
364. Engler, A.J.; Sen, S.; Sweeney, H.L.; Discher, D.E. Matrix elasticity directs stem cell lineage specification. *Cell* **2006**, *126*, 677–689. [CrossRef] [PubMed]
365. Soares, J.; Araujo, G.R.d.S.; Santana, C.; Matias, D.; Moura-Neto, V.; Farina, M.; Frases, S.; Viana, N.B.; Romão, L.; Nussenzveig, H.M.; et al. Membrane elastic properties during neural precursor cell differentiation. *Cells* **2020**, *9*, 1323. [CrossRef]
366. Zhang, R.; Jo, J.-I.; Kanda, R.; Nishiura, A.; Hashimoto, Y.; Matsumoto, N. Bioactive polyetheretherketone with gelatin hydrogel leads to sustained release of bone morphogenetic protein-2 and promotes osteogenic differentiation. *Int. J. Mol. Sci.* **2023**, *24*, 12741. [CrossRef]
367. Cazzanelli, P.; Wuertz-Kozak, K. MicroRNAs in intervertebral disc degeneration, apoptosis, inflammation, and mechanobiology. *Int. J. Mol. Sci.* **2020**, *21*, 3601. [CrossRef]
368. Tuna, R.; Yi, W.; Crespo Cruz, E.; Romero, J.; Ren, Y.; Guan, J.; Li, Y.; Deng, Y.; Bluestein, D.; Liu, Z.L.; et al. Platelet biorheology and mechanobiology in thrombosis and hemostasis: Perspectives from multiscale computation. *Int. J. Mol. Sci.* **2024**, *25*, 4800. [CrossRef] [PubMed]
369. Bryniarska-Kubiak, N.; Basta-Kaim, A.; Kubiak, A. Mechanobiology of dental pulp cells. *Cells* **2024**, *13*, 375. [CrossRef]
370. Minami, K.; Mori, T.; Nakanishi, W.; Shigi, N.; Nakanishi, J.; Hill, J.P.; Komiyama, M.; Ariga, K. Suppression of myogenic differentiation of mammalian cells caused by fluidity of a liquid–liquid interface. *ACS Appl. Mater. Interfaces* **2017**, *9*, 30553–30560. [CrossRef]
371. Jia, X.; Minami, K.; Uto, K.; Chang, A.C.; Hill, J.P.; Nakanishi, J.; Ariga, K. Adaptive liquid interfacially assembled protein nanosheets for guiding mesenchymal stem cell fate. *Adv. Mater.* **2020**, *32*, 1905942. [CrossRef]
372. Jia, X.; Song, J.; Lv, W.; Hill, J.P.; Nakanishi, J.; Ariga, K. Adaptive liquid interfaces induce neuronal differentiation of mesenchymal stem cells through lipid raft assembly. *Nat. Commun.* **2022**, *13*, 3110. [CrossRef]
373. Ueki, T.; Uto, K.; Yamamoto, S.; Tamate, R.; Kamiyama, Y.; Jia, X.; Noguchi, H.; Minami, K.; Ariga, K.; Wang, H.; et al. Ionic liquid interface as a cell scaffold. *Adv. Mater.* **2024**, *36*, 2310105. [CrossRef]
374. Chrysanthou, A.; Kanso, H.; Zhong, W.; Shang, L.; Gautrot, J.E. Supercharged protein nanosheets for cell expansion on bioemulsions. *ACS Appl. Mater. Interfaces* **2023**, *15*, 2760–2770. [CrossRef]
375. Peng, L.; Nadal, C.; Gautrot, J.E. Growth of mesenchymal stem cells at the surface of silicone, mineral and plant-based oils. *Biomed. Mater.* **2023**, *18*, 035005. [CrossRef] [PubMed]
376. Nomura, K.; Ohta, H.; Takagi, A.; Kamiya, T.; Hirano, M.; Hosono, H. Room-temperature fabrication of transparent flexible thin-film transistors using amorphous oxide semiconductors. *Nature* **2004**, *432*, 488–492. [CrossRef]
377. Sun, Z.; Chen, S.; Zhang, L.; Huang, R.; Wang, R. The understanding and compact modeling of reliability in modern metal–oxide–semiconductor field-effect transistors: From single-mode to mixed-mode mechanisms. *Micromachines* **2024**, *15*, 127. [CrossRef]
378. Fu, Y.; Liu, Z.; Yue, S.; Zhang, K.; Wang, R.; Zhang, Z. Optical second harmonic generation of low-dimensional semiconductor materials. *Nanomaterials* **2024**, *14*, 662. [CrossRef]
379. Kasuya, N.; Tsurumi, J.; Okamoto, T.; Watanabe, S.; Takeya, J. Two-dimensional hole gas in organic semiconductors. *Nat. Mater.* **2021**, *20*, 1401–1406. [CrossRef]
380. Kumagai, S.; Makita, T.; Watanabe, S.; Takeya, J. Scalable printing of two-dimensional single crystals of organic semiconductors towards high-end device applications. *Appl. Phys. Express* **2022**, *15*, 030101. [CrossRef]
381. Murai, M.; Iba, S.; Hamao, S.; Kubozono, Y.; Ota, H.; Takai, K. Azulene-fused linearly π-extended polycyclic aromatic compounds: Synthesis, photophysical properties, and OFETs applications. *Bull. Chem. Soc. Jpn.* **2023**, *96*, 1077–1081. [CrossRef]
382. Yamashita, Y.; Tsurumi, J.; Ohno, M.; Fujimoto, R.; Kumagai, S.; Kurosawa, T.; Okamoto, T.; Takeya, J.; Watanabe, S. Efficient molecular doping of polymeric semiconductors driven by anion exchange. *Nature* **2019**, *572*, 634–638. [CrossRef] [PubMed]

383. Watanabe, K.; Miura, N.; Taguchi, H.; Komatsu, T.; Nosaka, H.; Okamoto, T.; Yamashita, Y.; Watanabe, S.; Takeya, J. Improvement of contact resistance at carbon electrode/organic semiconductor interfaces through chemical doping. *Appl. Phys. Express* **2022**, *15*, 101005. [CrossRef]
384. Yamashita, Y.; Kohno, S.; Longhi, E.; Jhulki, S.; Kumagai, S.; Barlow, S.; Marder, S.R.; Takeya, J.; Watanabe, S. N-type molecular doping of a semicrystalline conjugated polymer through cation exchange. *Commun. Mater.* **2024**, *5*, 79. [CrossRef]
385. Ishii, M.; Yamashita, Y.; Watanabe, S.; Ariga, K.; Takeya, J. Doping of molecular semiconductors through proton-coupled electron transfer. *Nature* **2023**, *622*, 285–291. [CrossRef] [PubMed]
386. Ramprasad, R.; Batra, R.; Pilania, G.; Mannodi-Kanakkithodi, A.; Kim, C. Machine learning in materials informatics: Recent applications and prospects. *npj Comput. Mater.* **2017**, *3*, 54. [CrossRef]
387. Liang, Y.; Jiao, C.; Zhou, P.; Li, W.; Zang, Y.; Liu, Y.; Yang, G.; Liu, L.; Cheng, J.; Liang, G.; et al. Highly efficient perovskite solar cells with light management of surface antireflection. *Bull. Chem. Soc. Jpn.* **2023**, *96*, 148–155. [CrossRef]
388. Wang, Z.-L.; Funada, T.; Onda, T.; Chen, Z.-C. Knowledge extraction and performance improvement of Bi_2Te_3-based thermoelectric materials by machine learning. *Mater. Today Phys.* **2023**, *31*, 100971. [CrossRef]
389. Saito, N.; Nawachi, A.; Kondo, Y.; Choi, J.; Morimoto, H.; Ohshima, T. Functionalgroup evaluation kit for digitalization of information on the functional group compatibility and chemoselectivity of organic reactions. *Bull. Chem. Soc. Jpn.* **2023**, *96*, 465–474. [CrossRef]
390. Liao, T.; Xia, W.; Sakurai, M.; Wang, R.; Zhang, C.; Sun, H.; Ho, K.-M.; Wang, C.-Z.; Chelikowsky, J.R. Magnetic iron-cobalt silicides discovered using machine-learning. *Phys. Rev. Mater.* **2023**, *7*, 034410. [CrossRef]
391. Chaikittisilp, W.; Yamauchi, Y.; Ariga, K. Material evolution with nanotechnology, nanoarchitectonics, and materials informatics: What will be the next paradigm shift in nanoporous materials? *Adv. Mater.* **2022**, *34*, 2107212. [CrossRef] [PubMed]
392. Oviedo, L.R.; Oviedo, V.R.; Martins, M.O.; Fagan, S.B.; da Silva, W.L. Nanoarchitectonics: The role of artificial intelligence in the design and application of nanoarchitectures. *J. Nanopart. Res.* **2022**, *24*, 157. [CrossRef]
393. Lombardo, D.; Kiselev, M.A.; Magazù, S.; Calandra, P. Amphiphiles self-assembly: Basic concepts and future perspectives of supramolecular approaches. *Adv. Condens. Matter Phys.* **2015**, *2015*, 151683. [CrossRef]
394. Crupi, V.; Jannelli, M.P.; Magazu, S.; Maisano, G.; Majolino, D.; Migliardo, P.; Sirna, D. Rayleigh wing and Fourier transform infraredstudies of intermolecular and intramolecularhydrogen bonds in liquid ethylene glycol. *Mol. Phys.* **1995**, *84*, 645–652. [CrossRef]
395. Caccamo, M.T.; Magazù, S. Thermal restraint on PEG-EG mixtures by FTIR investigations and wavelet cross-correlation analysis. *Polym. Test.* **2017**, *62*, 311–318. [CrossRef]
396. Caccamo, M.T.; Mavilia, G.; Mavilia, L.; Lombardo, D.; Magazù, S. Self-assembly processes in hydrated montmorillonite by FTIR investigations. *Materials* **2020**, *13*, 1100. [CrossRef] [PubMed]
397. Zheng, W.; Yang, X.-L.; Wu, G.-Y.; Cheng, L. Controlled self-assembly of metallacycle-bridged gold nanoparticles for surface-enhanced Raman scattering. *Chem. Eur. J.* **2020**, *26*, 11695–11700. [CrossRef] [PubMed]
398. Wu, G.-Y.; Liang, C.; Li, H.; Zhang, X.; Yao, G.; Zhu, F.-F.; Hu, Y.-X.; Yin, G.-Q.; Zheng, W.; Lu, Z. A multi-responsive supramolecular heparin-based biohybrid metallogel constructed by controlled self-assembly based on metal–ligand, host–guest and electrostatic interactions. *Org. Chem. Front.* **2021**, *8*, 4715–4722. [CrossRef]
399. Wu, G.-Y.; Zheng, W.; Yang, X.-L.; Liu, Q.-J.; Cheng, L. Supramolecular metallacycle-assisted interfacial self-assembly: A promising method of fabricating goldnanoparticle monolayers with precise interparticlespacing for tunable SERS activity. *Tetrahedron Lett.* **2022**, *94*, 153716. [CrossRef]